의학박사 학위논문

Development of multi-dimensional diagnostic and prognostic models in epithelial ovarian cancer

상피성 난소암의 진단 및 예후 예측을 위한 다차원 모델 개발 연구

2021 년 2 월

서울대학교 대학원
의학과 산부인과학 전공
김 세 익

A Thesis for the Degree of Doctor of Philosophy

Development of multi-dimensional diagnostic and prognostic models in epithelial ovarian cancer

February 2021

Department of Obstetrics and Gynecology,

Seoul National University

College of Medicine

Se Ik Kim

상피성 난소암의 진단 및 예후 예측을 위한 다차원 모델 개발 연구

지도교수 송 용 상

이 논문을 의학박사 학위논문으로 제출함
2020 년 10 월

서울대학교 대학원
의학과 산부인과학 전공
김 세 익

김세익의 의학박사 학위논문을 인준함
2021년 1월

위 원 장 정 현 훈 (인)
부위원장 [illegible] (인)
위 원 노 재 홍 (인)
위 원 백 재 성 (인)
위 원 안 태 진 (인)

Development of multi-dimensional diagnostic and prognostic models in epithelial ovarian cancer

By

Se Ik Kim

A thesis submitted to Department of Medicine in partial fulfillment of the requirements for the Degree of Doctor of Philosophy in Medicine (Obstetrics and Gynecology) at Seoul National University

January 2021

Approved by Thesis Committee:

Professor Hyun Hoon Chung Chairman

Professor Yong Sang Song Vice chairman

Professor Jae Hong No

Professor Taesung Park

Professor Taejin Ahn

Abstract

Development of multi-dimensional diagnostic and prognostic models in epithelial ovarian cancer

Se Ik Kim
Department of Obstetrics and Gynecology,
Seoul National University College of Medicine

Ovarian cancer, one of the deadliest female cancers, shows the lowest 5-year survival rate among gynecologic malignancies. Owing to the absence of cancer-specific symptoms and effective screening tools, ovarian cancer tends to be diagnosed at an advanced-stage and thus has a high recurrence and mortality rate despite intensive treatment. Currently, cytoreductive surgery followed by taxane- and platinum-based chemotherapy is conducted as the primary treatment in patients with advanced-stage epithelial ovarian cancer. Nevertheless, 80% of patients who showed complete response after the primary treatment eventually experience the disease recurrence.

In keeping with the era of precision medicine, discovery of precise diagnostic models for ovarian cancer and models predicting the exact prognosis of epithelial ovarian cancer is necessary as the first step of implementation of individualized treatment. Thus, we conducted a series of studies developing various models in epithelial ovarian cancer.

In **chapter 1**, we developed a diagnostic model identifying ovarian cancer from benign ovarian tumors using metagenomic data from serum microbe-derived extracellular vesicles (EVs).

For women with adnexal masses, distinguishing ovarian cancer from benign ovarian tumors is an important issue, as it determines the treatment plan, including the surgical approach. The detection tools currently available for

ovarian cancer are serum cancer antigen 125 (CA-125) and imaging studies, such as ultrasonography, computed tomography (CT) scans, and magnetic resonance imaging (MRI). However, further improvements in differentiating adnexal masses are still needed.

In this study, we obtained serum samples from 166 patients with pathologically confirmed OC and 76 patients with benign ovarian tumors. For model construction and validation, samples were randomly divided into training and test sets in the ratio 2:1. Isolation of microbial EVs from serum samples of the patients and 16S rDNA amplicon sequencing were carried out. Metagenomic and clinicopathologic data-based ovarian cancer diagnostic models were constructed in the training set and then validated in the test set. There were significant differences in the metagenomic profiles between the OC and benign ovarian tumor groups; specifically, genus *Acinetobacter* was significantly more abundant in the ovarian cancer group. More importantly, *Acinetobacter* was the only common genus identified by seven different statistical analysis methods. Among the various metagenomic and clinicopathologic data-based ovarian cancer diagnostic models, the model consisting of age, serum CA-125 levels, and relative abundance of *Acinetobacter* showed the best diagnostic performance with the area under the receiver operating characteristic curve (AUC) of 0.898 and 0.846 in the training and test sets, respectively. Thus, our findings establish a metagenomic analysis of serum microbe-derived EVs as a potential tool for the diagnosis of ovarian cancer.

In **chapter 2**, we developed nomograms predicting treatment response and prognosis of epithelial ovarian cancer.

To date, several prognostic indexes and predictive nomograms for the survival outcome of epithelial ovarian cancer have been developed based on pre-operative imaging such as CT scans, differential blood cell counts, tumor markers, operative findings, or pathologic results. However, these nomograms were developed in different disease settings, analyzed only fragments of clinicopathologic factors, and had a low or limited prediction ability making it

difficult for physicians to use them in clinical practice. Thus, this study aimed to develop more precise nomograms to predict treatment response and survival outcomes in patients with epithelial ovarian cancer from two high-volume tertiary institutional hospitals through a comprehensive review of medical records and statistical analyses. All previously published and possible prognostic factors were included as far as possible and investigated.

In total, 866 patients diagnosed with and treated for epithelial ovarian cancer were included. To construct predictive nomograms for platinum sensitivity, 3-year progression-free survival (PFS), and 5-year overall survival (OS), we performed stepwise variable selection by measuring AUC with leave-one-out cross-validation. For model validation, 10-fold cross-validation was applied. The median length of observation was 42.4 months (interquartile range, 25.7 to 69.9 months), during which 441 patients (50.9%) experienced disease recurrence. The median value of PFS was 32.6 months and 3-year PFS rate was 47.8%, while 5-year OS rate was 68.4%. The AUCs of the newly developed nomograms predicting platinum sensitivity, 3-year PFS, and 5-year OS were 0.758, 0.841, and 0.805, respectively. We also developed predictive nomograms confined to the patients who underwent primary debulking surgery. The AUCs for platinum sensitivity, 3-year PFS, and 5-year OS were 0.713, 0.839, and 0.803, respectively. In conclusion, we successfully developed nomograms predicting treatment response and prognosis of patients with epithelial ovarian cancer. These nomograms are expected to be useful in clinical practice and in designing clinical trials.

In **chapter 3**, we investigated the impact of sarcopenia and body composition on survival outcomes in patients with advanced-stage high-grade serous ovarian carcinoma (HGSOC).

Sarcopenia, characterized by loss of skeletal muscle mass and function, and its impact on cancer prognosis may vary by geographical regions and ethnicities. Recently, quantitative analysis of biomedical images, referred to as radiomics, is emerging as a promising approach to facilitate clinical decisions and improve patient stratification. A cross-sectional image of CT scans at the level of the

third lumbar vertebra (L3) is known to represent an individual's body composition, such as total body skeletal muscle and adipose tissues and fat distribution.

We retrospectively identified patients diagnosed with and treated for International Federation of Gynecology and Obstetrics stage III-IV HGSOC. Skeletal muscle index (SMI) was measured using pre-treatment CT scans at the level of L3 vertebral body. Sarcopenia was defined as SMI <39.0 cm^2/m^2. Patients' clinicopathologic characteristics and survival outcomes were compared according to sarcopenia presence. For subgroup analysis, we also measured the total fat area from the same image. In total, 76 and 103 patients were assigned to the sarcopenia and control groups, respectively. Comorbidities, stage, serum CA-125 levels, and size of residual tumor after surgery were similar between both groups. After a median follow up of 42.7 months, both groups showed similar PFS and OS. In subgroup analysis confined to the sarcopenia group, patients with high fat-to-muscle ratio (FMR; ≥2.1, n=38) showed significantly worse OS than those with low FMR (<2.1, n=38) (5-year survival rate, 44.7% vs. 80.0%; *P*=0.046), whereas PFS was not different (*P*=0.365). Multivariate analyses identified high FMR as an independent poor prognostic factor for OS in this group (adjusted hazard ratio, 3.377; 95% confidence interval, 1.170–9.752; *P*=0.024). In conclusion, sarcopenia did not influence recurrence rates and survival in Korean patients with advanced-stage HGSOC. However, among the patients with sarcopenia, high FMR was associated with decreased OS.

From these integrative analyses, we successfully developed multi-dimensional diagnostic and prognostic models, consisting of individual's clinicopathologic, metagenomics, and radiomics data, in epithelial ovarian cancer. The multi-dimensional approach in epithelial ovarian cancer improved the predictive ability of each model and was found to be critical in precision cancer medicine. This approach will provide us with a therapeutic strategy, thereby allowing us to take a giant leap forward for individualized treatment of ovarian cancer.

……

Keywords: **ovarian cancer; high-grade serous carcinoma; diagnosis; prognosis; treatment response; survival; extracellular vesicle; microbiome; metagenomic analysis; sarcopenia; body composition.**

Student number**: 2014-30620**

Table of contents

List of figures and table

Figures

Tables

List of abbreviations

ANCOM: analysis of composition of microbiomes

AUC: area under the receiver operating characteristic curve

BMI: body mass index

CA-125: cancer antigen 125

CLR Perm: centered log-ratio transformation and permutation logistic regression model

CT: computed tomography

EV: extracellular vesicles

FIGO: International Federation of Gynecology and Obstetrics

FMR: fat-to-muscle ratio

HE4: human epididymis protein 4

HGSOC: high-grade serous ovarian carcinoma

HU: Hounsfield unit

IDS: interval debulking surgery

MLR: monocyte-to-lymphocyte ratio

MRI: magnetic resonance imaging

NAC: neoadjuvant chemotherapy

NHIS: National Health Insurance System

NLR: neutrophil-to-lymphocyte ratio

OECD: Organisation for Economic Co-operation and Development

OS: overall survival

OTU: operational taxonomic unit

PDS: primary debulking surgery

PFS: progression-free survival

PLR: platelet-to-lymphocyte ratio

PRR: platinum-resistant recurrence

PSR: platinum-sensitive recurrence

RECIST: Response Evaluation Criteria in Solid Tumors

RMI: risk of malignancy index

ROMA: risk of ovarian malignancy algorithm

SMI: skeletal muscle index

SVR: skeletal muscle mass-to-visceral fat ratio

VSR: visceral-to-subcutaneous fat ratio

ZIBSeq: zero-inflated beta regression

ZIG: zero-inflated Gaussian mixture model

Chapter I: Metagenomic analysis of serum microbe-derived extracellular vesicles and diagnostic models for ovarian cancer

1. Introduction

Ovarian cancer is the deadliest gynecologic cancer worldwide (1). In the United States, the number of new cases of ovarian cancer and cancer deaths from ovarian cancer in 2019 were estimated to be 22,530 (2.5% of all female cancers) and 13,980 (4.9% of female cancer deaths), respectively (2). In Korea, the incidence of ovarian cancer has been increasing gradually (3). Owing to a lack of specific symptoms and effective screening tools, the majority of ovarian cancer cases are diagnosed at an advanced stage, resulting in a high recurrence and mortality rate (4). Among the various histologic types of ovarian cancer, the majority (90%) are epithelial ovarian cancer.

For women with adnexal masses, distinguishing ovarian cancer from benign ovarian tumors is an important issue, as it determines the treatment plan, including the surgical approach. The detection tools currently available for ovarian cancer are serum cancer antigen 125 (CA-125) levels, ultrasonography, computed tomography (CT) scans, and magnetic resonance imaging (MRI). Combinations of modalities provide better diagnostic performance for identifying ovarian cancer than each modality alone (5). The risk of malignancy index (RMI) scoring system, consisting of serum CA-125, menopausal status, and ultrasound features, as well as the risk of ovarian malignancy algorithm (ROMA), a biomarker-based algorithm consisting of serum CA-125 and human epididymis protein 4 (HE4), have been developed (6, 7). Both RMI and ROMA are reliable tools and perform equally well in differentiating ovarian cancer from adnexal masses (8, 9). However, considering that their diagnostic

performance and accuracy differ among the prospective cohort studies, further improvements in differentiating adnexal masses are still needed (10-12).

Microbiota, a microbial environmental factor that we are constantly exposed to, has emerged as a link between the host and various cancer types. Human microbiome studies have revealed that significant differences in microbiota composition are associated with oral, esophageal, pancreatic, and colorectal cancers (13-16). Although the exact underlying mechanisms are still not well-understood, microbe-induced inflammation is thought to trigger changes in the tumor microenvironment, promoting tumorigenesis (17, 18). Advances in the sequencing technique of microbial genomes have expanded microbiome data and extended our understanding on microbiota-host interactions. Especially, 20–200 nanometer-sized extracellular vesicles (EVs), constitutively secreted by microbes and detectable in body fluids, are considered to play an important role in such interactions (19, 20).

A recent study has compared the microbiome signature between fresh ovarian cancer tissues (n=25) and normal fallopian tube fimbria tissues (n=25) and suggested that changes in microbial composition might be related to the process of ovarian cancer development (21). However, the relationship between serum microbial EVs and ovarian cancer has yet to be investigated. The relative abundance of certain microbial EVs released in the blood might differ between benign and malignant ovarian tumors, and those differences could be utilized in the differential diagnosis of adnexal masses. Thus, this study aimed at developing diagnostic models to differentiate between ovarian cancer and

benign ovarian tumors through the metagenomic analysis of serum microbial EVs.

2. Materials and Methods

2.1 Study population

Since June 2012, we have been collecting biological samples of patients scheduled to undergo surgery for adnexal masses for research purposes; under the patients' written informed consent, blood samples and cancer tissues are obtained the day before surgery and at the time of surgery, respectively, and then stored at the Human Biobank of Seoul National University Hospital (SNUH).

For the present study, we identified relevant patients and obtained their frozen serum samples from the Human Biobank. Inclusion criteria for the study population were as follows: (1) older than 18 years; (2) underwent surgery for an adnexal mass between June 2012 and February 2018; and (3) pathologically diagnosed with either epithelial ovarian cancer or benign ovarian tumor. Patients with the following conditions were excluded: (1) diagnosed with any malignancy other than ovarian cancer synchronously or before the surgery; (2) neoadjuvant chemotherapy (NAC) or targeted therapy before surgery; (3) borderline ovarian tumors; and (4) severe comorbidities, such as end-stage renal disease, uncontrolled diabetes mellitus, or long-term corticosteroid use.

In total, 166 patients with ovarian cancer and 76 patients with benign ovarian tumors were included in this study. Through review of the medical records, we

collected baseline characteristics including the age at diagnosis, body mass index (BMI), comorbidities, and initial serum CA-125 levels. We also reviewed all patients' pathology results and collected information on the International Federation of Gynecology and Obstetrics (FIGO) stage for the study group. Then, the patients' clinicopathologic characteristics were compared between the ovarian cancer group and the benign ovarian tumor group. Metagenomic profiling was carried out with the patients' frozen serum samples according to the procedures described below.

2.2 EV isolation and DNA extraction from serum samples

We isolated EVs from the serum samples using the differential centrifugation method, as described previously (22). In brief, serum samples were centrifuged at 3,000 rpm for 15 min at 4℃, and 100 ul of the supernatant was mixed with 1 × PBS, pH 7.4 (ML 008-01, Welgene, Republic of Korea). The floating particles were sunk through centrifugation at 10,000 *g* for 1 min at 4℃. After centrifugation, bacteria and foreign particles were thoroughly eliminated by sterilizing the supernatant through a 0.22-um filter.

To extract the DNA from the EVs' membranes, EVs separated from serum in the previous steps were boiled for 40 min at 100℃. To eliminate the remaining floating particles and debris, the supernatant was collected after 13,000 rpm of centrifugation for 30 min at 4℃. EVs' DNA was extracted using a DNA isolation kit according to the standard protocol (PowerSoil DNA Isolation Kit, MO BIO, Carlsbad, CA, USA). The DNA from EVs in each sample was quantified by using the QIAxpert system (QIAGEN, Hilden, Germany).

2.3 Microbial metagenomic analysis

16S rDNA gene-based metagenomic analysis, bacterial genomic DNA was amplified with 16S_V3_f (5′-TCGTCGGCAGCGTCAGATGTGTATAAGAG ACAGCCTACGGGNGGCWGCAG-3′) and 16S_V4_r (5′-GTCTCGTGGGC TCGGAGATGTGTATAAGAGACAGGACTACHVGGGTATCTAATCC-3′) primers, which are specific for the V3-V4 hypervariable regions of the 16S rDNA gene. The libraries were prepared using PCR products according to the MiSeq System guide (Illumina, San Diego, CA, USA) and quantified using a QIAxpert (QIAGEN, Hilden, Germany). Each amplicon was then quantified, and the equimolar ratio was set, pooled, and sequenced on a MiSeq (Illumina, San Diego, CA, USA) according to the manufacturer's recommendations.

2.4 Analysis of microbial composition in the microbiota

Paired-end reads that matched the adapter sequences were trimmed by Cutadapt (version 1.1.6) (23). The resulting FASTQ files containing paired-end reads were merged with CASPER and then quality filtered with Phred (Q) score-based criteria described by Bokulich (24, 25). Any reads shorter than 300 bp after merging were also removed. To identify the chimeric sequences, a reference-based chimera detection step was conducted with VSEARCH against the Greengenes database (26). Next, the sequence reads were clustered into operational taxonomic units (OTUs) using CD-HIT with a de novo clustering algorithm under a threshold of 97% sequence similarity. The representative

sequences of the OTUs were finally classified using the Greengenes database (version 13.8) with UCLUST (parallel_assign_taxonomy_uclust.py script on QIIME (version 1.9.1) under default parameters) (27). The Chao indices, an estimator of the richness of taxa per individual, were estimated to measure the diversity of each sample.

2.5 Development of diagnostic models for ovarian cancer

To construct and validate the diagnostic models for ovarian cancer, we randomly divided the samples from each group into training and test sets in the ratio 2:1, considering the ratio of ovarian cancer and benign ovarian tumors in the total 242 samples. The values of each training and test set were transformed to a centered log ratio. Discovery of microbiome biomarkers and construction of diagnostic models were performed in the training set (n=161), while validation of newly developed diagnostic models were performed in the test set (n=81).

We filtered the genus if the zero proportion was more than 99%. To identify specific microbiome biomarkers that were differentially distributed between the ovarian cancer and benign ovarian tumor groups, we performed metagenomic analyses using eight statistical methods popularly used with the filtered count data: Wilcoxon, Metastats, EdgeR, DESeq2, zero-inflated Gaussian mixture model (ZIG), zero-inflated beta regression (ZIBSeq), analysis of composition of microbiomes (ANCOM), and centered log-ratio transformation and permutation logistic regression model (CLR Perm). We used the abundance of the OTUs as the algorithms were developed based on the abundance data.

Comparing the list of significant microbiome biomarkers identified by each statistical method, we chose biomarkers that overlapped as far as possible, because each method provides a different list of microbiome biomarkers, and most overlapped ones are expected to be highly plausible biomarkers.

We constructed several diagnostic models identifying ovarian cancer from benign ovarian tumors by combining the microbiome biomarkers with patients' ages and serum CA-125 levels, and these models were validated in the test set. To evaluate the diagnostic performance of the developed models, each model's sensitivity, specificity, and area under the receiver operating characteristic curve (AUC) were calculated.

2.6 Statistical analysis

Statistical analyses were performed to evaluate differences in the clinicopathologic characteristics between the two groups. The Student's *t*-test and Mann–Whitney U test were used to compare continuous variables, while the Pearson's chi-square test and Fisher's exact test were used to compare categorical variables. Shannon index was calculated to measure α-diversities of the microbiota.

Summaries of the eight statistical methods that were applied to the metagenomic analyses are as follows: (1) The Wilcoxon rank sum test is the nonparametric type of the two-sample *t*-test, which uses the sum of ranks for observations. (2) Metastats compares the number of samples by group and the number of taxa. Welch's *t*-test statistics were applied when the taxon count was larger than the number of samples. Otherwise, Fisher's exact test was used. (3)

EdgeR and (4) DESeq2 methods are usually used in the analysis of RNA-sequencing data. As metagenome data is extracted from 16S rDNA, application of these methods has been often tried. Both methods are the negative binomial models; however, the difference between the two methods is that EdgeR uses a trimmed mean of M-values normalization, whereas DESeq2 uses a relative log expression normalization. (5) ZIG uses the log normal mixture model for the taxon count, taking sparsity on the OTU table into account. To overcome high false-positive rates, we adopted empirical Bayes shrinkage of parameter estimates. (6) ZIBSeq uses the beta mixture model for relative abundance. Relative abundance after total sum-scaling normalization was performed owing to the large number of zeros and results with the skewed distribution. (7) ANCOM was used to compare relative abundance of the OTUs; Wilcoxon rank sum test was used in comparisons of the two groups after the log-ratio transformation of all pairwise taxa. The Kruskal-Wallis test was used in comparisons of the three groups, and the Freidman test was used in comparisons of repetitive data. (8) CLR Perm fits the logistic model after the centered log-ratio transformation with count data to alleviate the sum to one constraint of relative abundance. The permutation test was adopted to decrease the false discovery rate.

R statistical software (version 3.4.4; R Foundation for Statistical Computing, Vienna, Austria; ISBN 3-900051-07-0; http://www.R-project.org) was used for the statistical analyses. A two-sided *P* value below 0.05 was considered statistically significant.

2.7 Ethical statement

This retrospective case-control study using metagenomics was conducted after obtaining approval from the Institutional Review Board of Seoul National University Hospital (SNUH; No. 1612-102-816).

3. Results

3.1 Characteristics of the study population

The overall study design is displayed in **Figure 1**. **Table 1** presents the clinicopathologic characteristics of all patients. Although patients in the ovarian cancer group were significantly older than those in the benign ovarian tumor group (mean, 53.6 vs. 49.4 years; P=0.041), other characteristics such as BMI, menopausal status, and comorbidities were similar. After 2:1 random distribution of the patients into training and test sets, ovarian cancer patients were still older than those with benign ovarian tumors in the training set, whereas patients' ages were similar in the test set. Both in the training and test sets, no differences in BMI, menopausal status, and comorbidities were observed between the ovarian cancer and benign ovarian tumor groups.

In the training set, serum CA-125 levels were significantly higher in patients with ovarian cancer (median, 331.1 vs. 22.3 IU/mL; P<0.001). Among the 110 patients with ovarian cancer, 39 (35.5%) and 71 (64.5%) were diagnosed with FIGO stage I-II and III-IV, respectively. The most common histologic type was high-grade serous carcinoma, which was observed in 54.5% of ovarian cancer patients. Among the 51 patients with benign ovarian tumor, mucinous

cystadenoma (47.1%) was the most common pathologic diagnosis, followed by serous cystadenoma (15.7%).

In the test set, the ovarian cancer group also showed significantly higher serum CA-125 levels compared to the benign ovarian tumor group (median, 432.3 vs. 20.6 IU/mL; P <0.001). FIGO stage I-II disease was observed in 41.1% of ovarian cancer patients. The most common histologic types in the ovarian cancer and benign ovarian tumor groups were high-grade serous carcinoma (50.0%) and serous cystadenoma (28.0%), respectively.

3.2 Comparison of metagenomics profiles between the two groups

Figure 2 depicts the landscape of the metagenomic profiles of all patients. **Figure 2A** shows all 31 phyla detected in ovarian cancer and benign ovarian tumor groups. In the genus-level composition, a total of 587 genera were detected in all patients. Among them, 110 significantly differentially distributed genera identified by at least two statistical methods are displayed with their relative abundance in **Figure 2B**. Herein, genus *Acinetobacter* showed high relative abundances both in ovarian cancer and benign ovarian tumor groups. In the training set, 107 of 110 ovarian cancer patients (97.3%) had *Acinetobacter*, while 50 of 51 benign ovarian tumor patients (98.0%) had *Acinetobacter*. In the test set, *Acinetobacter* was found in 98.2% (55/56) and 100.0% (25/25) of ovarian cancer and benign ovarian tumor groups, respectively.

In general, “genus” is regarded as the lowest level of taxonomy, where unassigned or unclassified microbiome are relatively small. Most previous studies on microbiome analyses have reported metagenomic profiles up to the genus level. Therefore, we investigated further metagenomic profiles of the two groups in the genus level.

In metagenomics, α-diversity and β-diversity are used to overview the distribution of the data composition: α-diversity refers to the richness, evenness, and dominance of taxa in a particular community, while β-diversity means taxonomic differences between the communities (28). Comparing the genus-level α-diversity, the Shannon index was not different between the ovarian cancer and benign ovarian tumor groups in the training set (median, 3.294 vs. 3.263; P=0.270), as well as in the test set (median, 3.210 vs. 3.238; P=0.810) (**Figure 3**). In order to compare β-diversity, we analyzed clustering at the genus level using multidimensional plots. However, these plots did not show distinguished clustering between the ovarian cancer and benign ovarian tumor groups in the training and test sets (**Figure 4**).

3.3 Development of diagnostic models for ovarian cancer

Through the metagenomic analyses using various statistical methods, we identified genus-level microbiome biomarkers that were differentially distributed between the ovarian cancer and benign ovarian tumor groups with statistical significance: Wilcoxon test, Metastats, EdgeR, DESeq2, ZIG, ZIBSeq, ANCOM, and CLR Perm identified 1, 98, 3, 8, 447, 56, 1, and 2 biomarkers, respectively, at adjusted q values using a false discovery rate

(≤0.05). **Table 2** shows the top 10 microbiome biomarkers identified by each statistical method, in order of overlap.

Next, we examined the overlap of these genus-level microbiome biomarkers among the eight statistical methods (**Figure 5**). In total, 486 biomarkers were identified to be significantly differentially distributed by at least one statistical method. Among them, 110 and nine markers overlapped at least two and three statistical methods, respectively. *Acinetobacter* was the only common genus identified by seven different statistical analysis methods. Specifically, *Acinetobacter* was significantly more abundant in the ovarian cancer group than in the benign ovarian tumor group (median [interquartile range], 0.084 [0.037–0.222] vs. 0.033 [0.008–0.075]; Wilcoxon rank sum test, P <0.001). Therefore, we selected *Acinetobacter* as the most potential and highly plausible genus-level microbiome biomarker for differentiating ovarian cancer from benign ovarian tumors.

Combining the relative abundance of *Acinetobacter* with patients' clinicopathologic variables, we constructed several diagnostic models to differentiate ovarian cancer from benign ovarian tumors (**Table 3**). The model composed of age, serum CA-125 levels, and relative abundance of *Acinetobacter* showed 86.4% sensitivity and 78.4% specificity. This model showed a superior AUC (0.898) than any other models, with less than three of the following variables: age, serum CA-125 levels, and *Acinetobacter*.

3.4 Validation of diagnostic models for ovarian cancer

The developed diagnostic models were validated in the test set. Among the

various models, the model consisting of patients' ages at diagnosis, initial serum CA-125 levels, and relative abundance of *Acinetobacter* yielded the best diagnostic performance for differentiating ovarian cancer from benign ovarian tumors as follows: sensitivity, 82.1%; specificity, 68.0%; and AUC, 0.846 (**Table 3** and **Figure 6**).

4. Discussion

In the present study, we successfully extracted microbe-derived EVs from the serum samples and characterized the metagenomic profiles of 242 patients: 166 with ovarian cancer and 76 with benign ovarian tumors. Incorporating the relative abundance of specific microbiomes at the genus level with patients' ages and serum CA-125 levels, we developed a new diagnostic model to differentiate ovarian cancer from benign ovarian tumors; this model even showed a better diagnostic performance than those without a microbiome biomarker.

Recently, metagenomic analysis has been noticed as a new approach; it has opened new horizons in the diagnosis of human disease. The Human Microbiome Project, funded by the National Institutes of Health, triggered the broadening of our insights into the microbiome. The relative abundance of certain microbes varies in chronic diseases, such as diabetes, obesity, cardiovascular disease, inflammatory bowel disease, and chronic allergies (29, 30). In various malignancies, disruption in the stability of microbiota or structural microbiome shifts have been reported (13-16). However, to date, few studies have examined microbiomes in ovarian cancer (21).

The current study provides new scientific evidence regarding different distributions of microbiomes in serum EVs between ovarian cancer and benign ovarian tumors. Unlike previous researchers who used samples obtained from female reproductive organs (21, 31), we used patients' serum samples. Compared to the former, obtaining serum samples is much easier and less invasive; organ harvesting is not required. Considering the fact that an exact diagnosis is confirmed through surgery, a pre-operative diagnostic model using serum samples certainly has merit. Therefore, our study shows the potential of serum microbial EVs as a liquid biopsy for the diagnosis of ovarian cancer.

Interestingly, we found that the genus *Acinetobacter* was significantly more abundant in the ovarian cancer group than in the benign ovarian tumor group. Moreover, *Acinetobacter* was the only commonly found genus through almost all available statistical analysis methods developed so far. In general, *Acinetobacter baumannii* (*A. baumannii*), a species of the genus *Acinetobacter*, is a pathogen related to human infections, such as pneumonia, blood stream infection, urinary tract infection, and meningitis (32). Infection with *Acinetobacter* is also common in cancer patients, and a relationship between *A. baumannii* and poor survival outcomes was also reported among patients with various cancer types(33, 34). Similar to our study, Zhou et al. showed that *Acinetobacter*, especially the *Acinetobacter lwoffii* species, was significantly enriched in ovarian cancer tissues compared to normal distal fallopian tube tissues (21).

To explore the underlying mechanisms between *Acinetobacter* and epithelial ovarian cancer, the following two aspects should be considered: bacterial

factors and host responses against them. Bacterial products, such as lipopolysaccharide (LPS), can stimulate the tumor to produce proinflammatory cytokines that enhance tumor survival (LPS-induced tumor growth). On the host side, Toll-like receptors (TLRs) are transmembrane proteins known to play an important role in immunosurveillance and responses toward microorganisms (35).

Previously, through in vitro and in vivo studies, researchers have demonstrated that LPS, as well as EVs, secreted by *A. baumannii* stimulate the TLR-4 signaling pathway and trigger the host's immune response against an *A. baumannii* infection (36-39). In addition, EVs secreted by *Acinetobacter nosocomialis*, another important pathogen of various opportunistic infections, are also known to induce cytotoxicity of epithelial cells and host inflammatory responses (40). Interestingly, the expression of TLR-4 is observed in both the normal ovarian surface and epithelial ovarian tumor cell lines (41). In epithelial ovarian cancer, TLR-4 signaling has been demonstrated to promote tumor growth and to develop chemoresistance (42). Therefore, we suggest that products secreted by the *Acinetobacter* species may cause the development of epithelial ovarian cancer through the TLR-4 signaling pathway.

In accordance with the era of precision medicine, it is obvious that reliable diagnostic tools are essential for detecting ovarian cancer. Our study results imply that adding the metagenomic data to the conventional diagnostic model might improve its performance in the detection of ovarian cancer. However, the diagnostic model composed of patients' ages, serum CA-125 levels, and relative abundance of the genus *Acinetobacter* needs to be externally validated.

Nevertheless, this study tried to overcome this limitation by separating the test and training sets from the beginning and faithfully implementing the internal validation.

Developing the diagnostic models for identifying ovarian cancer, we believed that it was the most important to reduce the false-negative rate considering its worse prognosis compared to any other malignancies. Therefore, during the model construction, we focused on achieving a high accuracy and maintaining the sensitivity, even if specificity was compromised. As the result, we reported our newly developed diagnostic model's diagnostic performance as follows: sensitivity 86.4% and specificity 78.4% (AUC 0.898) in the training set; and sensitivity 82.1% and specificity 68.0% (AUC 0.846) in the test set.

Diagnostic performance of our newly developed, microbiome biomarker-based diagnostic model was not compared with the currently available tools, such as the ROMA and RMI scoring systems. At our institution, the serum HE4 test is not routinely performed in women with adnexal masses. In our study population, only 53.3% (129/242) underwent the serum HE4 test, so that ROMA could be calculated. Owing to the retrospective study design, we were not able to retrieve all the pre-operative transvaginal ultrasonography images, so that RMI scoring system could not be applied. Moreover, if microbiome biomarkers are integrated with ROMA or RMI, there is the possibility that the diagnostic performance for identifying ovarian cancer might be much improved. Now, we are planning a prospective cohort study to validate the clinical usefulness of the serum-based metagenomic analysis in the diagnosis of ovarian cancer. In that study, every single subject will undergo both ROMA and RMI

for further investigation.

The current study also has other limitations. First, the relationship between the microbiome and ovarian cancer should be further investigated. We do not know whether our findings could explain the pathogenesis of ovarian cancer or were just a phenomenon in this cohort. The cause-and-effect relationship between differing microbiome compositions and ovarian cancer should be investigated. Additional translational studies, such as hypothesis-proving cell-line or animal studies, are warranted. Second, the current study is a single-institution study requiring external validation in different study populations. For example, the proportion of clear cell carcinoma in the ovarian cancer group was relatively high: 16.4% and 19.6% in the training and test sets, respectively. In this study, all patients were Korean, and according to the literature on histologic types of epithelial ovarian cancer, ovarian clear cell carcinoma is more common in the East Asian population than in the Western population (43, 44). Therefore, ovarian cancer groups from other regions or ethnicities with different proportions of histologic types might have different metagenomic profiles of serum EVs. Third, the FIGO stage of the ovarian cancer cases was not considered in developing the diagnostic models. Approximately 30% of ovarian cancer patients in our study population had FIGO stage I disease. The extent of disease might affect the composition of the serum microbe-derived EVs. Therefore, it is necessary to compare ovarian cancer patients' metagenomic profiles by stages in a large-sized cohort. Lastly, the sample size for the benign ovarian tumor group was small, which resulted in quite different histologic types between the training and test sets, although we randomly

divided the samples.

Despite these limitations, the current study was the first to characterize the metagenomic profiles of the serum microbial EVs in ovarian cancer. Through evaluation of the serum microbiomes, we were able to build a diagnostic model for ovarian cancer. The metagenomic analysis of serum microbiomes has several advantages, particularly the ease of sample collection, which suggests an increase of its usability.

In conclusion, we found that 16S rDNA gene-based metagenomic analyses revealed differences in the metagenomic profiles of serum microbial EVs between patients with ovarian cancer and those with benign ovarian tumors. We also developed a microbiome biomarker-based diagnostic model differentiating ovarian cancer from benign ovarian tumors and found that the serum microbiome may play a role in the early detection of ovarian cancer. Further prospective studies are warranted to validate these results.

Table 1. Patients' clinicopathologic characteristics

Characteristics	All (n=242, %)	Training Set			Test Set		
		Cancer (n=110, %)	Benign (n=51, %)	*P*	Cancer (n=56, %)	Benign (n=25, %)	*P*
Age, years							
Mean ± SD	52.3 ± 13.4	53.8 ± 12.3	48.2 ± 15.9	0.031	53.4 ± 11.5	51.8 ± 15.7	0.658
BMI, kg/m2							
Mean ± SD	23.0 ± 3.4	22.6 ± 3.1	23.1 ± 3.6	0.387	23.1 ± 3.6	23.9 ± 4.2	0.370
Menopause	141 (58.3)	68 (61.8)	26 (51.0)	0.194	34 (60.7)	13 (52.0)	0.463
Comorbidities							
Hypertension	55 (22.7)	27 (24.5)	8 (15.7)	0.205	11 (19.6)	9 (36.0)	0.115
Diabetes	21 (8.7)	11 (10.0)	6 (11.8)	0.735	1 (1.8)	3 (12.0)	0.085
Dyslipidemia	34 (14.0)	18 (16.4)	6 (11.8)	0.446	6 (10.7)	4 (16.0)	0.489
Serum CA-125, IU/mL							
Median (range)	126.3 (2.3–10000.0)	331.1 (2.3–10000.0)	22.3 (3.5–1821.0)	<0.001	432.3 (7.7–9909.0)	20.6 (5.7–1710.0)	<0.001
FIGO stage							
I	52 (21.5)	33 (30.0)			19 (33.9)		
II	10 (4.1)	6 (5.5)			4 (7.1)		
III	75 (31.0)	53 (48.2)			22 (39.3)		
IV	29 (12.0)	18 (16.4)			11 (19.6)		
Histologic type							
Epithelial ovarian cancer							
High-grade serous	88 (36.4)	60 (54.5)			28 (50.0)		
Low-grade serous	8 (3.3)	6 (5.5)			2 (3.6)		
Mucinous	15 (6.2)	10 (9.1)			5 (8.9)		
Endometrioid	16 (6.6)	9 (8.2)			7 (12.5)		

Clear cell	29 (12.0)	18 (16.4)	11 (19.6)	
Mixed	6 (2.5)	3 (2.7)	3 (5.4)	
Others	4 (1.7)	4 (3.6)	0	
Benign ovarian tumor				
Mucinous cystadenoma	28 (11.6)	24 (47.1)		4 (16.0)
With fibroma	5 (2.1)	4 (7.8)		1 (4.0)
Without fibroma	23 (9.5)	20 (39.2)		3 (12.0)
Serous cystadenoma	15 (6.2)	8 (15.7)		7 (28.0)
With fibroma	4 (1.7)	3 (5.9)		1 (4.0)
Without fibroma	11 (4.5)	5 (9.8)		6 (24.0)
Seromucinous cystadenoma	6 (2.5)	4 (7.8)		2 (8.0)
With fibroma	2 (0.8)	1 (2.0)		1 (4.0)
Without fibroma	4 (1.7)	3 (5.9)		1 (4.0)
Endometriotic cyst	8 (3.3)	4 (7.8)		4 (16.0)
Mature cystic teratoma	8 (3.3)	6 (11.8)		2 (8.0)
Fibroma/fibrothecoma	9 (3.7)	3 (5.9)		6 (24.0)
Paratubal cyst	2 (0.8)	2 (3.9)		0

Abbreviations: BMI, body mass index; CA-125, cancer antigen 125; FIGO, International Federation of Gynecology and Obstetrics; SD, standard deviation.

Table 2. Top 10 genus-level microbiome biomarkers significantly differentially distributed between the ovarian cancer and benign ovarian tumor groups

Genus	Wilcoxon	Metastats	EdgeR	DESeq2	ZIG	ZIBSeq	ANCOM	CLR Perm
Acinetobacter	<0.001	0.008	0.093	0.043	<0.001	<0.001	*Acinetobacter*	<0.001
Isoptericola	0.841	<0.001	0.487	1	0.046	<0.001	Not detected	0.855
Terrisporobacter	0.841	0.023	0.600	1	<0.001	<0.001	Not detected	0.944
SM1A02	0.989	0.008	0.528	1	<0.001	0.002	Not detected	0.935
Candidatus Alysiosphaera	0.841	<0.001	0.476	1	0.015	<0.001	Not detected	0.901
Ralstonia	0.841	<0.001	0.462	1	<0.001	0.005	Not detected	0.913
Hydrogenophaga	0.771	<0.001	0.872	1	<0.001	0.027	Not detected	0.809
Pseudorhodoferax	0.921	0.024	0.811	1	<0.001	0.007	Not detected	0.779
Bryobacter	0.841	0.023	0.420	1	0.007	0.999	Not detected	0.849
Varibaculum	0.841	0.013	0.600	1	0.599	<0.001	Not detected	0.416

Shown with the *q* values.

Table 3. Diagnostic models differentiating ovarian cancer from benign ovarian tumors

Model	Training Set			Test Set		
	Sensitivity	**Specificity**	**AUC**	**Sensitivity**	**Specificity**	**AUC**
Age	0.554	0.490	0.589	0.518	0.520	0.531
Age, CA-125	0.773	0.686	0.809	0.768	0.560	0.816
Age, *Acinetobacter*	0.827	0.529	0.770	0.839	0.440	0.667
Age, CA-125, *Acinetobacter*	0.864	0.784	0.898	0.821	0.680	0.846

Abbreviations: AUC, area under the receiver operating characteristic curve; CA-125, cancer antigen 125.

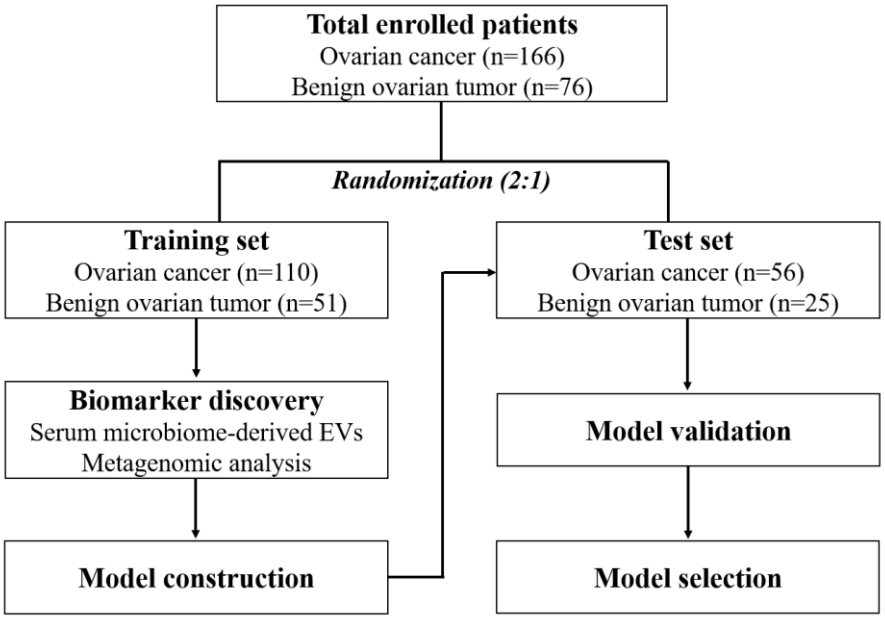

Figure 1. Flow diagram illustrating the overall study design.

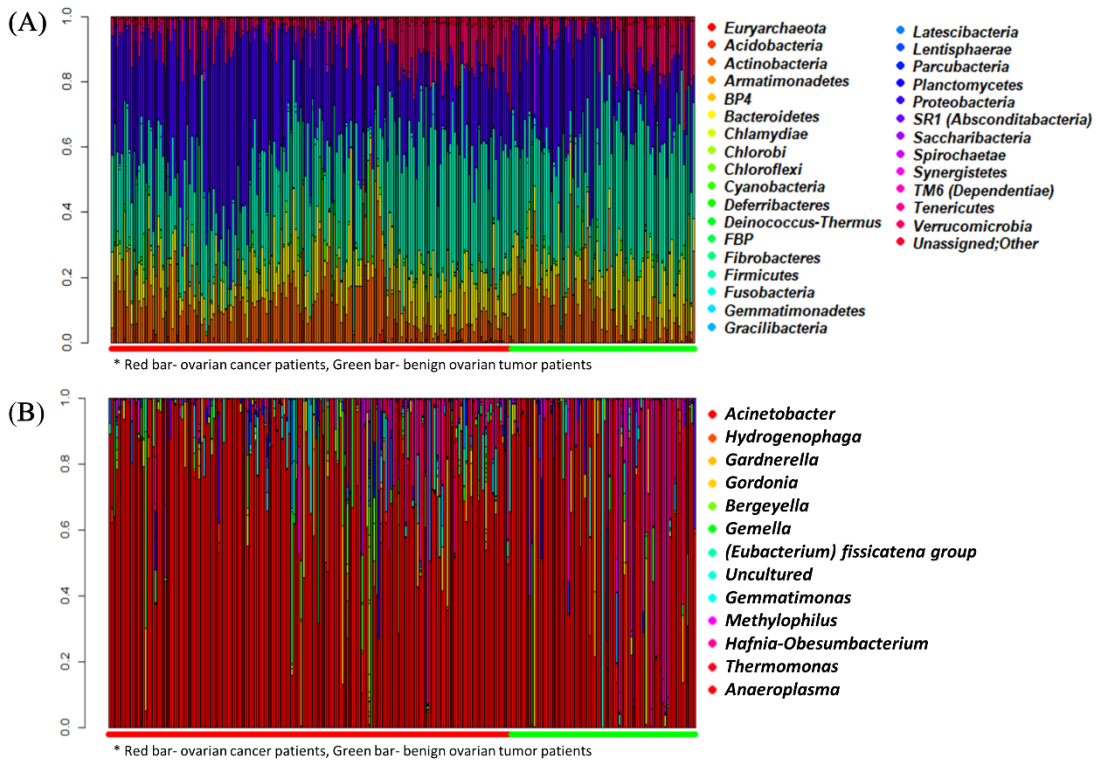

Figure 2. Landscape of metagenomic profiles in all patients. (A) Phylum-level composition. (B) Genus-level composition. Below the plot, red and green horizontal bars indicate ovarian cancer patients and benign ovarian tumor patients, respectively.

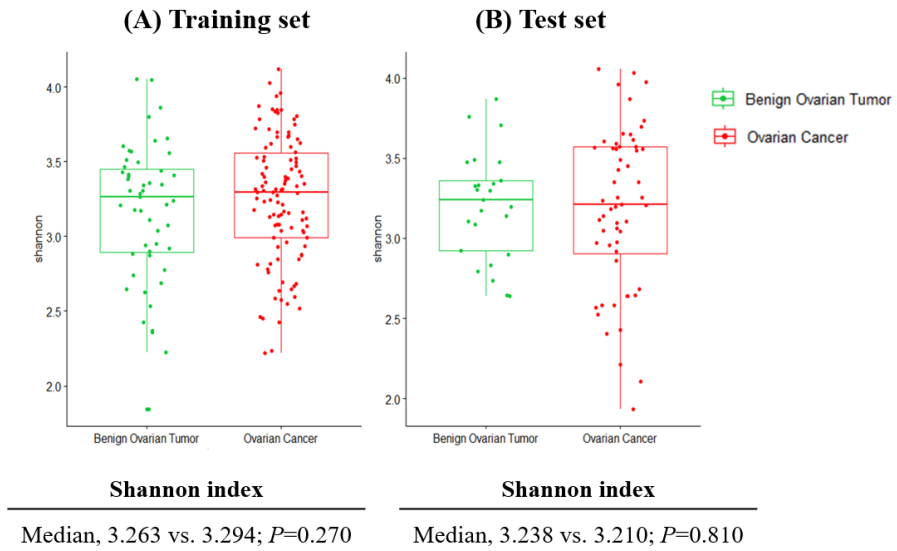

Figure 3. Comparisons of genus-level α-diversity between the two groups. (A) Training set. (B) Test set.

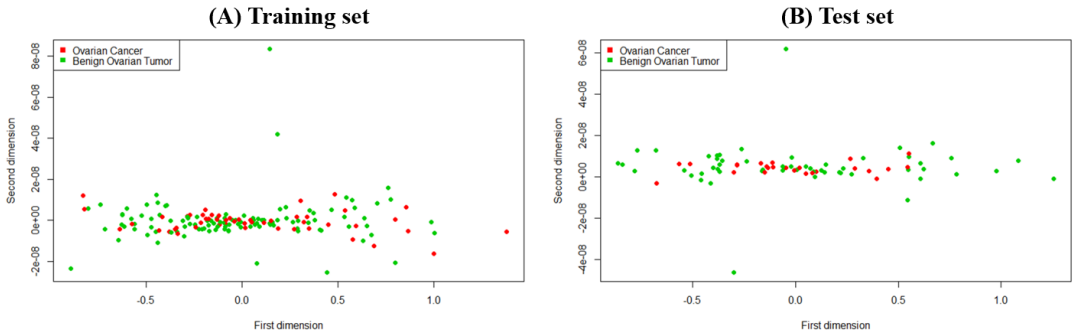

Figure 4. Genus-level multidimensional plots. (A) Training set. (B) Test set.

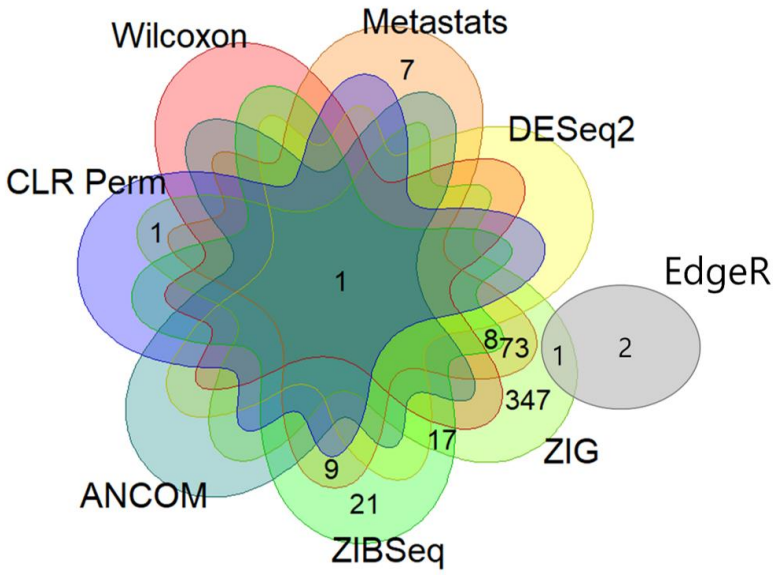

Figure 5. Selection of genus-level microbiome biomarkers. Venn diagram depicts the overlapping of biomarkers among the eight statistical methods.

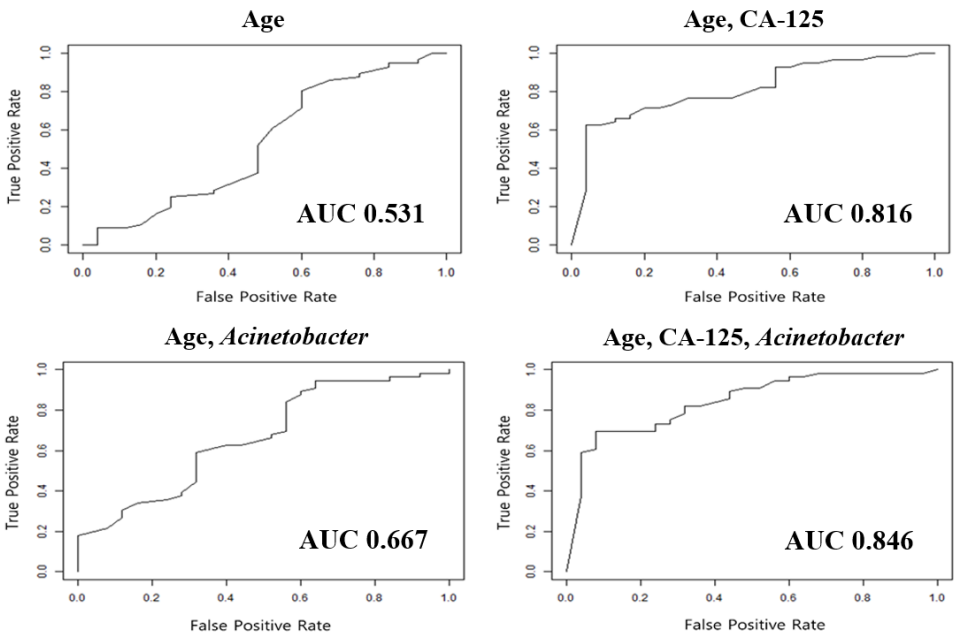

Figure 6. Comparisons of performances among diagnostic models differentiating ovarian cancer from benign ovarian tumors.

Chapter II: Development of nomograms to predict treatment response and prognosis of epithelial ovarian cancer

1. Introduction

Ovarian cancer, one of the deadliest female cancers, shows the lowest 5-year survival rate (46.5%) among gynecologic malignancies (2). The absence of cancer-specific symptoms and effective screening tools has led to high rates of ovarian cancer diagnosis in late stages, recurrence, and mortality (45). The majority (90%) of ovarian cancers are epithelial ovarian cancers (46). Maximal cytoreductive surgery followed by taxane- and platinum-based chemotherapy is conducted as the primary treatment in patients with advanced stage epithelial ovarian cancer (47-49) . Nevertheless, 80% of patients who showed complete response after the primary treatment eventually experience the disease recurrence (50).

In keeping with the era of precision medicine, discovery of models predicting the exact prognosis of epithelial ovarian cancer is necessary as the first step of implementation of individualized treatment. To date, several prognostic indexes and predictive nomograms for the survival outcome of epithelial ovarian cancer have been developed based on pre-operative imaging such as CT scans, differential blood cell counts such as platelet and neutrophil, tumor markers such as serum CA-125 levels, operative findings, or pathologic results (51-59). However, these nomograms were developed in different disease settings (primary or recurrent epithelial ovarian cancers), analyzed only fragments of clinicopathologic factors, and had a low or limited prediction ability making it difficult for physicians to use them in clinical practice. Moreover, the prediction of primary treatment response to divide patients into possible platinum-sensitive recurrence (PSR) or platinum-resistant recurrence (PRR) groups

would be useful in clinical trials on first and second-line treatments, reducing the relevant time and cost.

Thus, this study aimed to develop more precise nomograms to predict treatment response and survival outcomes in patients with epithelial ovarian cancer from two high-volume tertiary institutional hospitals through comprehensive review of medical records and statistical analyses. All previously published and possible prognostic factors were included as far as possible and investigated in the current study.

2. Materials and Methods

2.1 Study population

From the Ovarian Cancer Cohort Databases of two tertiary institutional hospitals, we included patients who met the following inclusion criteria: (1) patients older than 18 years of age; and (2) those with epithelial ovarian cancer diagnosed and primarily treated at SNUH or Asan Medical Center (AMC) between January 2007 and August 2016. However, we excluded patients with the following conditions: (1) patients with any malignancy other than epithelial ovarian cancer; and (2) those with insufficient clinical data. As a result, we enrolled 866 patients who met these criteria; 570 from SNUH and 296 from AMC (**Figure 7**).

2.2 Data collection

We collected a vast amount of patients' clinicopathologic data including 108

variables over 16 domains (**Figure 8**). Data acquisition included age, personal history, such as parity, familial history of breast cancer or gynecologic malignancies, and co-morbidities, such as hypertension or diabetes. Serum CA-125 levels and differential blood cell counts including neutrophil, lymphocyte, monocyte and platelet at initial diagnosis were obtained. FIGO stage, histology and tumor differentiation, as well as details of primary treatment including the use of NAC, extent and individual procedures of debulking surgery, and administration and cycles of post-operative taxane- and platinum-based chemotherapy, were also obtained. Residual tumor size and sites after debulking surgery were investigated, and optimal debulking surgery was considered when the size of the residual tumor was less than 1 cm at the longest diameter. Pre-operative imaging studies and intra-operative surgical findings were also investigated.

All patients underwent CT scans and measurement of serum CA-125 levels every 3 cycles during post-operative adjuvant chemotherapy, and every 3 months for 1 year, then every 6 months for next 3 years during surveillance after primary treatment. Reponses to chemotherapy were evaluated by Response Evaluation Criteria in Solid Tumors (RECIST) version 1.1 (60).

For the survival analyses, progression-free survival (PFS) was defined as the time that elapsed from the start of the primary treatment (the date of primary debulking surgery [PDS] or the date of the first cycle of NAC) to the date of disease progression as evaluated by RECIST version 1.1 in patients with measurable disease (60). In patients with unmeasurable disease, the Gynecologic Cancer InterGroup criteria using serum CA-125 levels were used

to confirm disease progression (61). Overall survival (OS) was defined as the time that elapsed from the date of initial diagnosis to the date of cancer-related death or end of the study. For all patients, the status of survival was investigated using both institutional medical records and the Social Security Death Index.

For the assessment of platinum sensitivity, only the patients who actually received taxane- and platinum-based chemotherapy as primary treatment were included. Among them, those who showed recurrence were classified into either PSR, defined as relapsing 6 months or more after completion of primary treatment, or PRR, defined as relapsing in less than 6 months. In addition to PSR, those who completed taxane- and platinum-based chemotherapy and did not experience disease recurrence for at least 6 months of the follow-up period were also considered platinum-sensitive.

2.3 Statistical analysis

The overall work flow of statistical analysis is depicted in **Figure 9**. In total, there were 86 clinical variables that could play a role as predictors of platinum sensitivity, 3-year PFS, and 5-year OS. After excluding 17 variables that had missing data in more than 10% of the patients or had sparse occurrence with observed counts of less than 10, we performed statistical analysis on the 69 remaining variables.

Some variables, such as serum CA-125 levels, were log transformed to alleviate the skewness. For the eight variables that needed proper categorizations (age, histology, involvement of the spleen, omentum, small bowel and mesentery, colon except rectosigmoid, and liver surface, and residual

tumor size after PDS or interval debulking surgery [IDS]), we selected the most suitable categorizations showing high statistical significances in univariate analyses. For platinum sensitivity, a logistic regression univariate model was used and for PFS and OS, Cox regression univariate models were used.

To exclude variables correlated with others, we selected a variable or a set of variables from the group as follows. Among weight, height, BMI, and categorized BMI, BMI was used in the analyses. Similarly, among hemoglobin, differential blood cell counts, and their calculated secondary values, including neutrophil to lymphocyte ratio, monocyte to lymphocyte ratio, and platelet to lymphocyte ratio, the following variables were selected: hemoglobin, platelet count, neutrophil count, lymphocyte count, and monocyte count.

Before building the prediction models, univariate analysis was performed to screen for candidate clinical variables. First, *P* value was applied with 0.05 as the cutoff since a variable with high AUC can be an important predictor only when it is statistically significant. Then, AUC was computed using the 10-fold cross-validation procedure and 0.55 was applied as the cutoff value. After screening, 26, 25, and 23 variables remained for the construction of models predicting platinum sensitivity, 3-year PFS, and 5-year OS, respectively.

To build the prediction models, a logistic regression model for platinum sensitivity and Cox regression models for PFS and OS were fitted in stepwise variable selection using the AUC. For Cox regression models, we constructed a time dependent receiver operating characteristic curve and calculated time-dependent AUC (62). AUC was computed by leave-one-out cross-validation as follows: we estimated the parameters of a model on n-1 samples and got a

prediction on the remaining one with the estimated parameters from n-1 samples, where n is the sample size. This was repeated on all the samples so that we had n predicted values based on n estimated models. We computed AUC using the predicted values and the observed values of the response variable. The reason why we used AUC rather than the *P* value, the Akaike's information criterion, or the Bayesian information criterion was that the aim of this study was to identify the model with the best prediction.

In order to select the first variable, we fitted as many univariate models as the number of predictors. For each variable, we computed AUC and selected the one with the highest AUC value. To search for the model with the highest AUC, we employed forward and backward stepwise selections Let $x_{(m)}$ be the variable to be selected at step m and S_m be the set which consists of $x_{(1),}\ldots, x_{(m)}$. Suppose AUC(S_{m-1}, x_i) represents AUC value using $\{S_{m-1}, x_i\}$.

(1) Forward step: For each $x_i \in S_{m-1}^C$, the complement set of S_{m-1}, AUC(S_{m-1}, x_i) was computed. Then, we selected x_i if AUC(S_{m-1}, x_i) was the highest and larger than AUC(S_{m-1}), and set $x_{(m)}= x_i$ and $S_m = S_{m-1} \cup \{x_{(m)}\}$. If there was no further selection, we proceeded to Step 3.

(2) Backward step: For each $x_i \in S_m$, AUC($S_m \setminus \{x_i\}$) was computed, where $S_m\setminus\{x_i\}$ represented the set S_m without x_i. We deleted x_i if AUC($S_m\setminus\{x_i\}$) was the highest and larger than AUC(S_m). If there was no further deletion, we proceeded to Step 3.

(3) Stop the stepwise method for variable selection.

The final models were used to construct nomograms for platinum sensitivity, 3-year PFS, and 5-year OS, respectively. To double-check the AUCs for the models, which were established from the stepwise selection by AUC using leave-one-out cross-validation, 10-fold cross-validation was applied.

All the statistical analyses were performed using the R statistical software version 3.4.3 (The R Foundation for Statistical Computing, Vienna, Austria; ISBN 3-900051-07-0; http://www.R-project.org). A *P* value of <0.05 was considered statistically significant.

2.4 Ethical statement

The study was approved by the Institutional Review Board of both SNUH (No. 1609-132-798) and AMC (No. 2017-0199) and performed in accordance with the principles of the Declaration of Helsinki. The informed consent was waived.

3. Results

3.1 Characteristics of the study population

The clinicopathologic characteristics of a total of 866 patients are presented in **Table 4**. The patients' mean age was 53.5 years. Overall, 584 patients (67.4%) had FIGO stage III-IV disease, and the most common histologic type was serous type (61.1%). Details of primary treatment are also shown in **Table 4**. A

total of 712 patients (82.2%) received PDS, whereas the other 154 (17.8%) received NAC followed by IDS. The rate of optimal debulking surgery was 90.3%. After surgery, 792 patients (91.5%) received post-operative taxane- and platinum-based chemotherapy. Among them, 616, 108 and 13 patients showed complete remission, partial remission and stable disease, respectively, whereas 55 patients showed progressive disease. **Table 5** depicts pre-operative and intraoperative findings according to the anatomic sites. Analysis for ascites of peritoneal washing cytology was performed in 785 patients (90.6%), and malignant cells were detected in 482 patients (55.7%). Meanwhile, 76 patients (8.8%) presented pleural effusion at the time of diagnosis.

3.2 Patients' survival outcomes and treatment response

The median duration of follow-up for the 866 patients was 42.4 months (interquartile range, 25.7 to 69.9 months), during which 441 patients (50.9%) experienced disease recurrence. OS and PFS of the patients are displayed in **Figure 10**. The median OS was not reached, while the median PFS was 32.6 months. The 5-year OS and 3-year PFS rates were 68.4% and 47.8%, respectively.

Survival outcomes according to the FIGO stage are presented in **Figure 11**. Significant differences were observed in OS (P <0.001), as well as in PFS (P <0.001), according to the FIGO stage. The 5-year OS rates for FIGO stage I-II and stage III-IV were 91.9% and 55.8%, respectively, and the 3-year PFS rates were 84.9% and 30.6%, respectively. For stage III-IV, the median OS was 76.8 months and the median PFS was 17.9 months.

We also performed survival analyses according to the primary treatment strategies. Patients in the PDS group showed significantly better OS (5-year survival rates, 73.3% vs. 45.6%; P <0.001) and PFS (median, 59.6 vs. 15.9 months; P <0.001) compared to those in the NAC group (**Figure 12**).

Among the recurred (n=441), 433 patients (98.2%) had received post-operative taxane- and platinum-based chemotherapy: in all, 285 patients and 148 patients were PSR and PRR, respectively. In the assessment of platinum sensitivity, 562 (64.9%) and 148 (17.1%) were classified as platinum-sensitive and -resistant patients, respectively (**Table 4**).

3.3 Development of predictive nomograms

Using the statistical method described above, the nomograms were developed. **Figures 13, 14,** and **15** depict the developed nomograms for platinum sensitivity, 3-year PFS, and 5-year OS, respectively.

The nomogram for predicting platinum sensitivity included the following variables: log serum CA-125 levels at diagnosis, FIGO stage, histologic type, NAC, pleural effusion, ascites or peritoneal washing cytology, involvement of the omentum, uterus, colon except rectosigmoid, and liver surface, and residual tumor size after debulking surgery. The AUC of this model was 0.758.

By the same algorithm, a nomogram for the prediction of 3-year PFS was developed. It was composed of hemoglobin, lymphocyte count, monocyte count, and log serum CA-125 levels at diagnosis, ascites or peritoneal washing cytology, NAC, involvement of the ovarian surface, tube, omentum, and small

bowel and mesentery, and residual tumor size after PDS/IDS, with an AUC value of 0.841.

The newly developed nomogram for predicting 5-year OS consisted of lymphocyte count, monocyte count, log serum CA-125 levels, pleural effusion, ascites or peritoneal washing cytology, NAC, and involvement of the uterus, tube, omentum, colon except sigmoid, and small bowel and mesentery, with an AUC value of 0.805.

We performed 10-fold cross-validation to compute the AUCs of the nomograms for platinum sensitivity, 3-year PFS, and 5-year OS from stepwise selection by AUC using leave-one-out cross-validation. The values of AUC of the proposed nomograms were 0.743, 0.841, and 0.810 for platinum sensitivity, 3-year PFS, and 5-year OS, respectively. These values were similar to those we estimated by leave-one-out cross-validation.

Finally, we fitted a user-friendly interface on the developed nomograms and posted them onto a website to facilitate clinical use (http://statgen.snu.ac.kr/software/nomogramOvarian). These web-based nomograms consisted of an HTML file for the input of the risk factors and a CGI file for the output of the calculated results.

3.4 Development of nomograms excluding patients who underwent NAC

We also developed predictive nomograms using the same procedure confined to the patients who underwent PDS. For platinum sensitivity, the nomogram

consisted of hemoglobin, monocyte count, log serum CA-125 levels, pleural effusion, involvement of the uterus, omentum, and colon except rectosigmoid, and residual tumor size after PDS, with an AUC value of 0.713.

For 3-year PFS, the nomogram consisted of hemoglobin, lymphocyte count, monocyte count, segmented neutrophil count, FIGO stage, ascites or peritoneal washing cytology, and involvement of the tube, omentum, small bowel and mesentery, and large bowel resection with an AUC value of 0.839.

For 5-year OS, the nomogram included lymphocyte count, monocyte count at diagnosis, ascites or peritoneal washing cytology, and involvement of the tube, uterus, colon except sigmoid, and small bowel and mesentery with an AUC value of 0.803.

4. Discussion

In the present study, we successfully developed nomograms predicting platinum sensitivity, 3-year PFS, and 5-year OS of patients with epithelial ovarian cancer. The AUCs were calculated as 0.758, 0.841, and 0.805, respectively. To our knowledge, this is the first study developing predictive nomograms from two tertiary institutional hospitals in Korean patients with epithelial ovarian cancer.

In accordance with the era of precision medicine, demands on such predictive nomograms are increasing, and utilization of them will facilitate individualized treatment. As a nomogram visualizes the risks or benefits intuitively, a clinically relevant nomogram will be a useful tool during consultation between physicians and patients in clinical practice. For example, if an epithelial ovarian

cancer patient was identified at high risk for recurrence or platinum resistance by our newly developed nomograms, she might undergo more aggressive treatments in addition to the standard treatment: intraperitoneal chemotherapy or bevacizumab maintenance treatment might be considered. Physicians might recommend her to receive germline *BRCA1/2* testing as early as possible, so as to prescribe poly(ADP-ribose) polymerase (PARP) inhibitors based on the test results. Beside these aggressive treatments, more frequent surveillance schedule might be provided to the patients for earlier detection of recurrence than by usual methods.

To date, several nomograms predicting survival prognosis of epithelial ovarian cancer have been developed in various disease settings. In 2007, a Japanese multicenter study proposed a prognostic index to predict OS in FIGO stage III-IV disease (51), while a Memorial Sloan-Kettering Cancer Center group published a nomogram predicting 5-year OS after PDS confined to bulky stage IIIC disease in 2008 (52). The same group further developed the nomogram, expanding it to the entire stage (54). A two-center study in the Netherlands proposed nomograms for PFS and OS in patients with advanced-stage epithelial ovarian cancer (53). An Australia research group used data from the CALYPSO trial and developed prognostic nomograms to predict platinum-sensitive recurrent epithelial ovarian cancer patients' PFS and OS in 2011 and 2013, respectively (55, 56). Previs et al. (57) performed a multicenter retrospective study and reported a nomogram predicting 5-year OS probability in recurrent epithelial ovarian cancer patients who received bevacizumab and chemotherapy. In their multivariate model, prior number of chemotherapy

regimens, treatment free interval, platinum sensitivity, and the presence of ascites were identified as prognostic variables (57). Recently, a nomogram for survival in PRR was also developed by reviewing medical records of 164 patients retrospectively (59). As described in the studies above, nomograms for epithelial ovarian cancer have been developed in different disease settings or study populations.

Compared to the previous studies, the current study had a different and more specific design. We confined the study population to those with epithelial ovarian cancer who received primary treatment in two tertiary institutional hospitals. We also collected a vast amount of patients' clinic-pathologic data, trying to include all the previously published and possible prognostic factors as possible. Keeping in mind that the newly developed nomograms should be utilized in clinical practice or designing clinical trials, pre-operative and intra-operative findings were systematically organized. At the time of statistical analyses, we tried to avoid analyzing only fragments of clinic-pathologic factors. Rather, we performed stepwise selection method to select variables.

During stepwise variable selection, we also computed AUCs by 10-fold cross-validation, which were utilized for selecting variables, and obtained prediction models. When we repeated these processes, we observed a big variation in the selected models. This might originate from the existence of variables with similar prediction abilities. To solve such big variations among the selected models, we applied leave-one-out cross-validation when we computed AUCs in variable selection. As a result, we were able to provide prediction models which do not depend on random partitioning. Such a clear

statistical method has contributed to increase the robustness and prediction accuracy of the developed model.

Interestingly, components of differential blood cell counts, as well as hemoglobin, were included in the nomograms as prognostic factors. In the nomogram for predicting 3-year PFS, hemoglobin, lymphocyte count, and monocyte count were included and in the nomogram for predicting 5-year OS, lymphocyte count and monocyte count were included. Among the previous studies on development of nomograms predicting prognosis of epithelial ovarian cancer, Gerestein et al. (53) reported that pre-operative platelet count was one of the prognostic factors for PFS, while pre-operative platelet count and serum hemoglobin concentration were prognostic factors for OS. In the retrospective study by Paik et al. (58), lymphocyte count and monocyte count were included in their nomogram for platinum sensitivity, while platelet count and neutrophil count were included in the nomograms for 3-year PFS and 5-year OS, respectively. It is well known that neutrophilic differentiation is induced by tumors through various chemokines, and is associated with angiogenesis and cell proliferation (63). However, the scientific evidence underlying differential blood cell counts and its impact on the prognosis of epithelial ovarian cancer still remains unclear.

The current study had several limitations. Firstly, owing to the retrospective study design, inevitable issues, such as selection bias, may exist. Secondly, the developed nomograms were only validated internally using cross-validation methods. Although the cross-validation is well-known and reasonable, external validation processes in large-sized cohorts are still warranted. Lastly, use of

targeted agents, such as bevacizumab, a monoclonal antibody targeting vascular endothelial growth factor A, and PARP inhibitors was not considered in this study because of very low proportions among the study population. In Korea, the National Health Insurance System (NHIS) started to cover bevacizumab in platinum-resistant relapsed epithelial ovarian cancer in August 2015 based on the results of the AURELIA trial (64), and in May 2018, started to cover bevacizumab in patients with PSR based on the OCEANS and GOG-0213 trials (65, 66). Meanwhile, although three recent randomized trials on maintenance therapy with three types of PARP inhibitors reported significantly improved PFS in platinum-sensitive relapsed epithelial ovarian cancer with *BRCA1/2* mutation, only olaparib has been covered by NHIS since October 2017 (67). If clinical data on these drugs accumulate, it would be worth developing a predictive nomogram for prognosis in epithelial ovarian cancer considering use of such drugs as variables.

Despite the study's limitations, strengths of this study are as follows: (1) the specific study design and statistical methodology allowed us to integrate and analyze epithelial ovarian cancer patients' clinicopathologic characteristics comprehensively, yielding valuable findings. (2) Compared to previously published studies, the sample size and the number of collected variables were larger in the current study. Especially, patients from two highest volume tertiary hospitals in Korea were included. Each hospital operates its own comprehensive cancer center. (3) Because we determined each patient's survival status by querying the Korean government's Social Security Death Index, survival data are very accurate. (4) Professional statisticians of the

research team analyzed vast amount of patients' data. Although policy for treatment of epithelial ovarian cancer is same, patients' data might be somehow heterogeneous. However, the statisticians combined them well and successfully performed statistical analyses. (5) Predictive nomograms for the patients who will undergo PDS were also developed.

In conclusion, we have successfully developed nomograms for predicting platinum sensitivity, 3-year PFS, and 5-year OS of patients with epithelial ovarian cancer. By providing the exact prognosis of epithelial ovarian cancer to the individual patients, the nomograms are expected to be useful in clinical practice and in conducting prospective cohort studies or designing clinical trials. Furthermore, if the multi-omics data of epithelial ovarian cancer patients are added onto the predictive models, we expect that the predictive ability of the model will increase.

Table 4. Patients' clinicopathologic characteristics

Characteristics	All (n=866, %)
Age, years	53.5 ± 11.2
BMI, kg/m2	23.4 ± 3.4
Co-morbidities	
Hypertension	
No	698 (80.6)
Yes	168 (19.4)
Diabetes	
No	797 (92)
Yes	69 (8)
Dyslipidemia	
No	803 (92.7)
Yes	61 (7.0)
Unknown	2 (0.2)
Pretreatment CBC	
Hemoglobin, g/dL	12.3 ± 1.3
Platelets, 10^3/uL	327.5 ± 104.2
WBC, 10^3/uL	7.1 ± 2.5
Segmented neutrophils, %	66.3 ± 10.1
Count, 10/uL	478.4 ± 215.3
Lymphocytes, %	24.3 ± 9.0
Count, 10/uL	160.2 ± 56.2
Monocytes, %	6.9 ± 2.3
Count, 10/uL	47.5 ± 23.4
Ln(CA-125), IU/ml	5.8 ± 1.9
FIGO stage	
I	220 (25.4)
II	62 (7.2)
III	441 (50.9)
IV	143 (16.5)
Histologic type	
Serous	529 (61.1)
Endometrioid	96 (11.1)
Mucinous	79 (9.1)
Clear cell	85 (9.8)
Others	77 (8.9)
Primary treatment strategy	
PDS	712 (82.2)
NAC	154 (17.8)

Residual tumor after PDS/IDS	
No gross	638 (73.7)
<1 cm	144 (16.6)
1 - 2 cm	44 (5.1)
>2 cm	31 (3.6)
Unknown	9 (1.0)
Post-operative taxane- and platinum-based chemotherapy	
No	74 (8.5)
Yes	792 (91.5)
CR*	616 (71.1)
PR	108 (12.5)
SD	13 (1.5)
PD	55 (6.4)
Recurrence	
No	425 (49.1)
Yes	441 (50.9)
No post-operative chemotherapy	8 (0.9)
PSR†	285 (32.9)
PRR	148 (17.1)
Platinum sensitivity	
Platinum-sensitive‡	562 (64.9)
Platinum-resistant	148 (17.1)

Values are presented as mean ± standard deviation or number (%).

Abbreviations: BMI, body mass index; CA-125, cancer antigen 125; CBC, complete blood count; WBC, white blood cell; FIGO, International Federation of Gynecology and Obstetrics; PDS, primary debulking surgery; NAC, neoadjuvant chemotherapy; IDS, interval debulking surgery; CR, complete remission; PR, partial remission; SD, stable disease; PD, progressive disease; PSR, platinum-sensitive recurrence; PRR, platinum-resistant recurrence.

*Reponses to chemotherapy were evaluated by Response Evaluation Criteria in Solid Tumors (RECIST) version 1.1.

†PSR was defined as relapse ≥6 months after completion of taxane- and platinum-based chemotherapy, whereas PRR as relapse <6 months.

‡In addition to PSR, the patients who completed taxane- and platinum-based chemotherapy and did not experience disease recurrence during at least 6 months of follow-up period were considered platinum-sensitive.

Table 5. Pre-operative and intra-operative findings

Characteristics	All (n=866, %)
Pleural effusion	
No	790 (91.2)
Yes	76 (8.8)
Cytology not performed	29 (3.3)
Negative for malignant cell	9 (1)
Positive for malignant cell	38 (4.4)
Ascites or peritoneal washing cytology	
Negative for malignant cell	303 (35.0)
Positive for malignant cell	482 (55.7)
Ovarian surface	
No involvement	245 (28.3)
Yes	581 (67.1)
Fallopian tube	
No involvement	451 (52.1)
Yes	391 (45.2)
Uterus	
No involvement	477 (55.1)
Yes	344 (39.7)
Colon except rectosigmoid colon	
No involvement	631 (72.9)
Yes	233 (26.9)
Omentum	
No involvement	439 (50.7)
≤ 2 cm	162 (18.7)
> 2 cm	263 (30.4)
Small bowel and mesentery	
No involvement	619 (71.5)
≤ 2 cm	194 (22.4)
> 2 cm	47 (5.4)
Liver surface	
No involvement	719 (83)
≤ 2 cm	108 (12.5)
> 2 cm	36 (4.2)

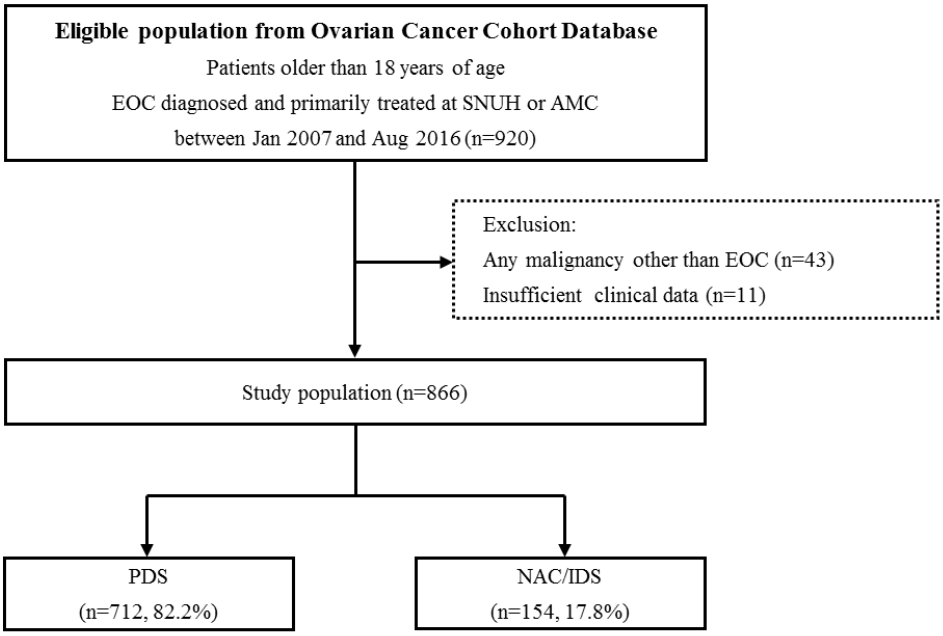

Abbreviations: EOC, epithelial ovarian cancer; SNUH, Seoul National University Hospital; AMC, Asan Medical Center; PDS, primary debulking surgery; NAC/IDS, neoadjuvnat chemotherapy followed by interval debulking surgery.

Figure 7. Flow diagrams depicting the selection of the study population.

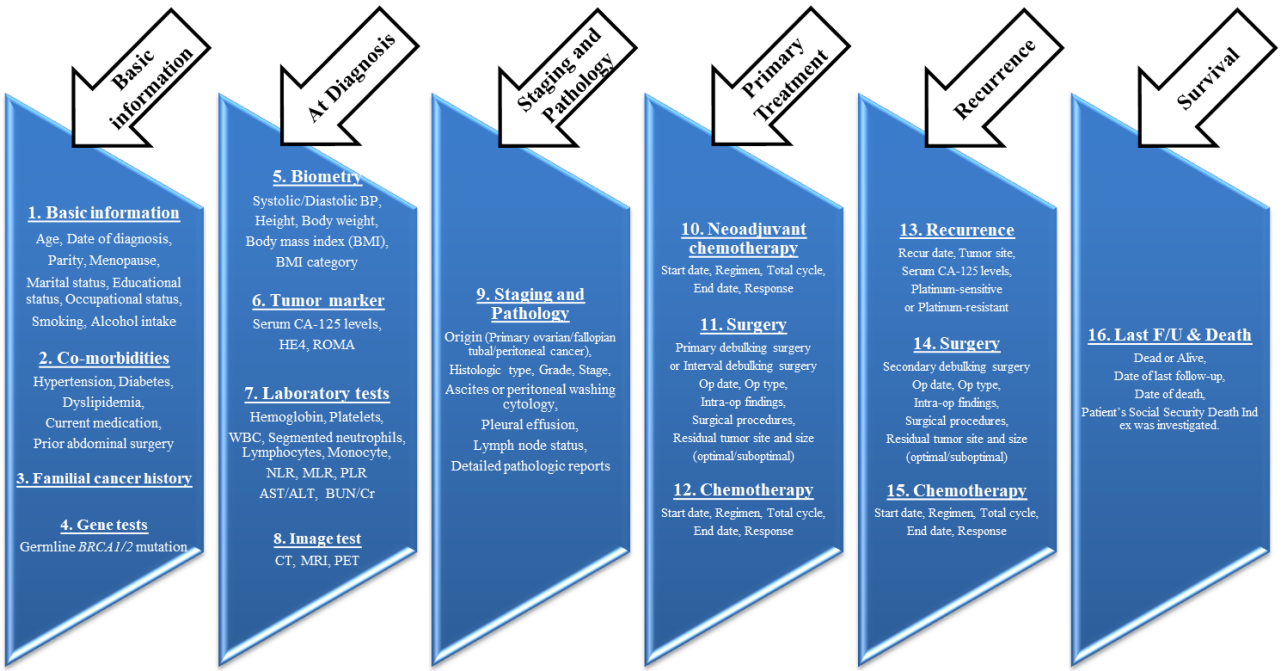

Figure 8. A scheme of data acquisition. Patients' clinicopathologic data included 108 variables over 16 domains.

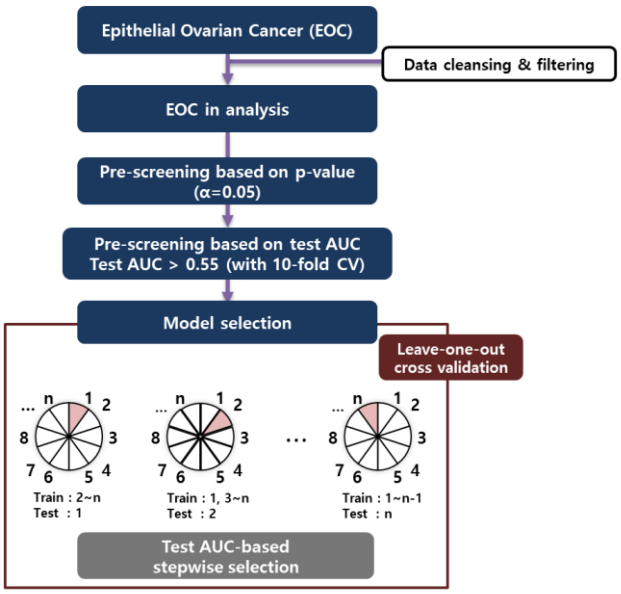

Figure 9. Overall work flow of statistical analysis.

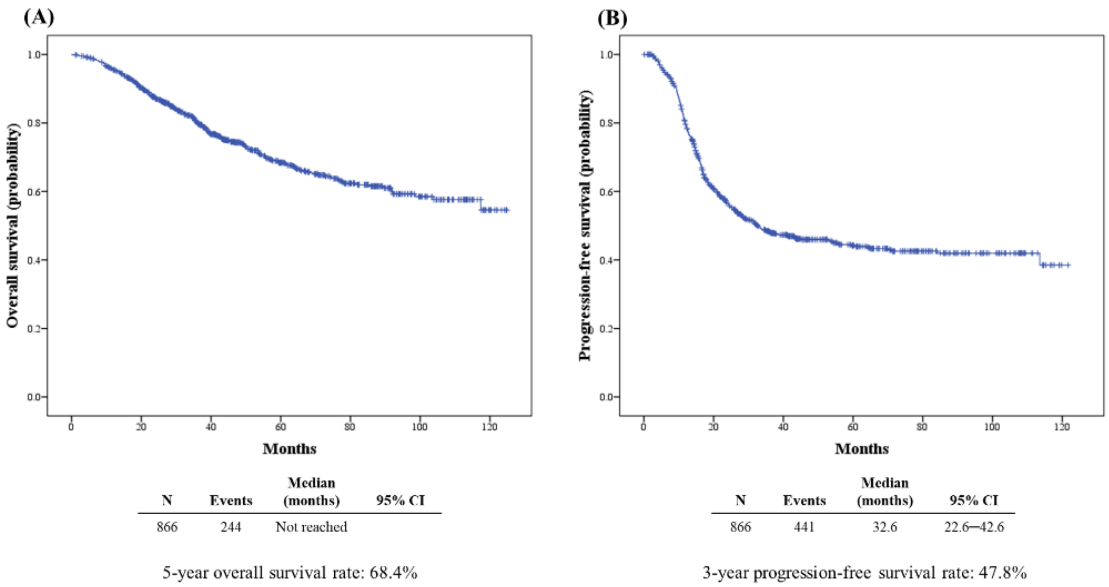

Figure 10. Survival outcomes of the study population. (A) Overall survival. (B) Progression-free survival.

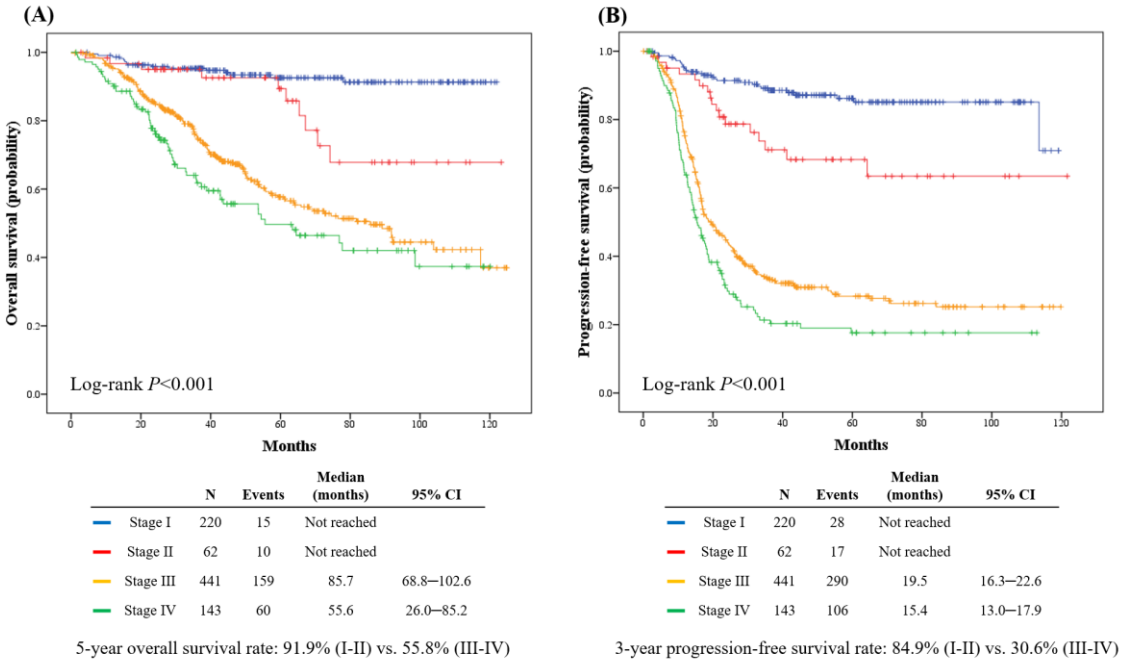

	N	Events	Median (months)	95% CI
Stage I	220	15	Not reached	
Stage II	62	10	Not reached	
Stage III	441	159	85.7	68.8–102.6
Stage IV	143	60	55.6	26.0–85.2

5-year overall survival rate: 91.9% (I-II) vs. 55.8% (III-IV)

	N	Events	Median (months)	95% CI
Stage I	220	28	Not reached	
Stage II	62	17	Not reached	
Stage III	441	290	19.5	16.3–22.6
Stage IV	143	106	15.4	13.0–17.9

3-year progression-free survival rate: 84.9% (I-II) vs. 30.6% (III-IV)

Figure 11. Survival outcomes according to the FIGO stage. (A) Overall survival. (B) Progression-free survival.

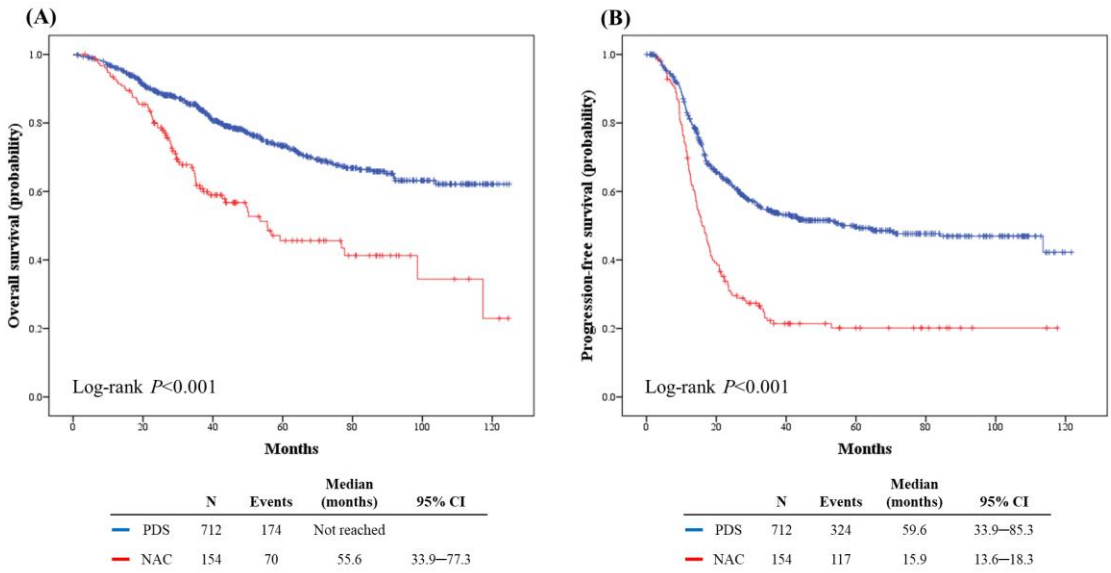

	N	Events	Median (months)	95% CI
PDS	712	174	Not reached	
NAC	154	70	55.6	33.9–77.3

5-year overall survival rate: 73.3% vs. 45.6%

	N	Events	Median (months)	95% CI
PDS	712	324	59.6	33.9–85.3
NAC	154	117	15.9	13.6–18.3

3-year progression-free survival rate: 54.0% vs. 22.3%

Figure 12. Survival outcomes according to the primary treatment strategy.
(A) Overall survival. (B) Progression-free survival.

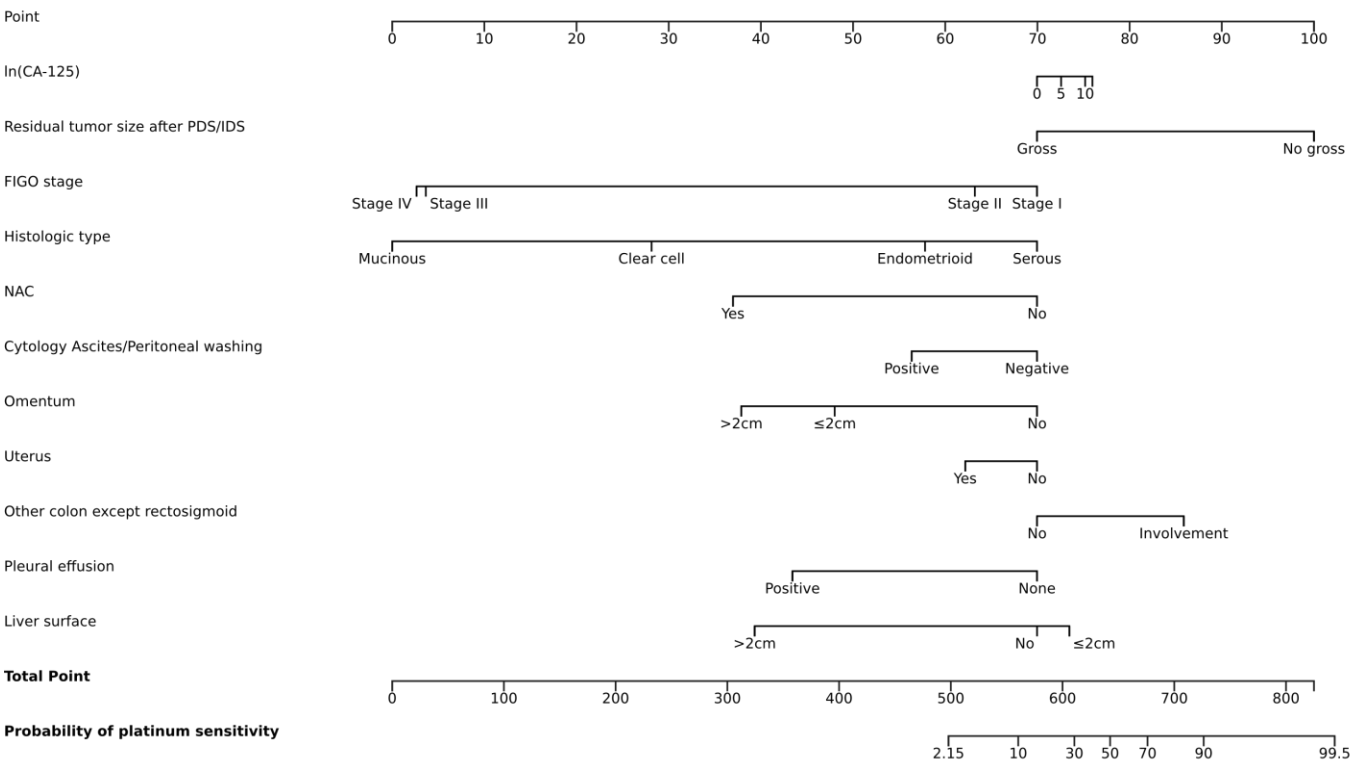

Figure 13. The developed nomogram predicting platinum sensitivity.

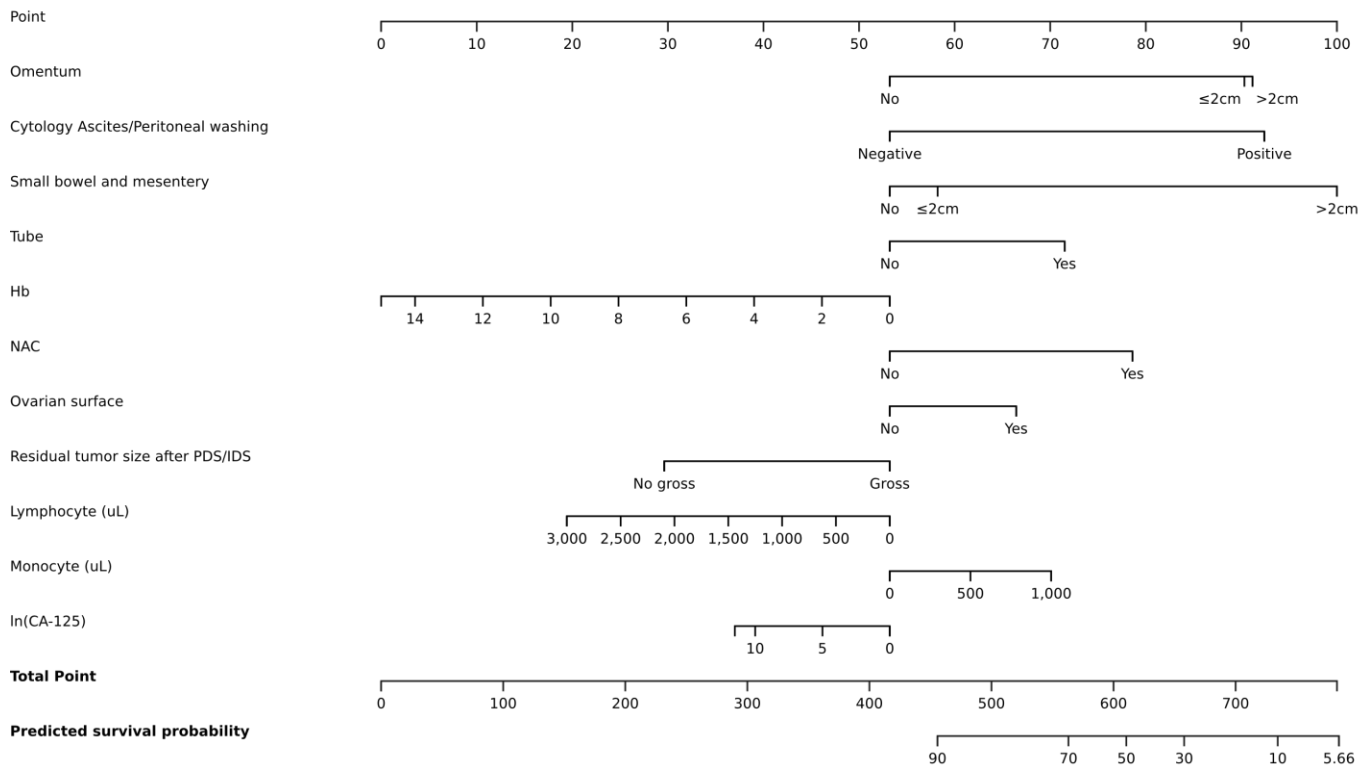

Figure 14. The developed nomogram predicting 3-year progression-free survival.

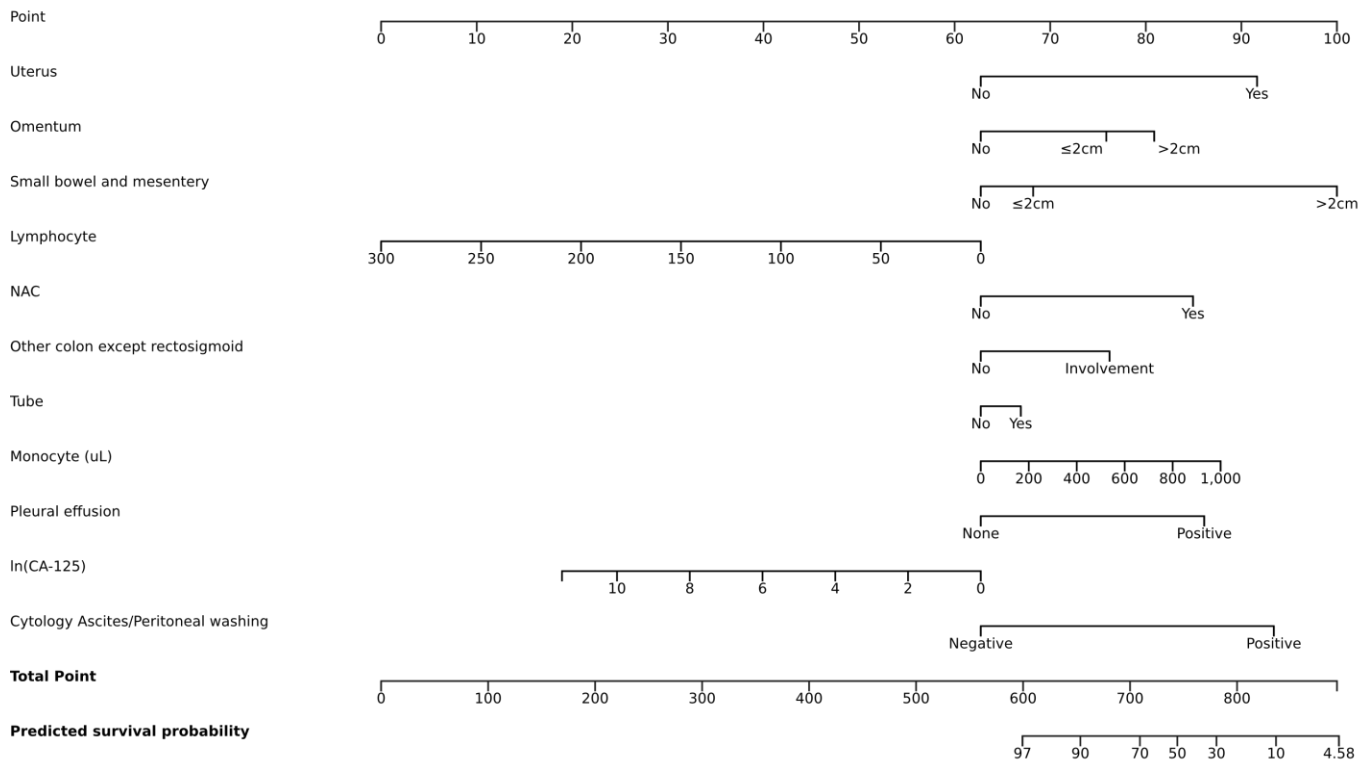

Figure 15. The developed nomogram predicting 5-year overall survival.

Chapter III: Body composition analysis in patients with advanced-stage high-grade serous ovarian carcinoma

1. Introduction

Ovarian cancer is one of the deadliest gynecologic malignancies (1). The incidence of ovarian cancer is higher among high Human Development Index countries, and it is gradually increasing in Korea (3). Owing to the absence of cancer-specific symptoms and effective screening tools, ovarian cancer tends to be diagnosed at an advanced-stage and thus has a high recurrence rate and poor 5-year survival rate despite intensive treatment (45).

Sarcopenia, characterized by loss of skeletal muscle mass and function, does not occur exclusively in the elderly but is also commonly observed in cancer patients (68). Previous studies have suggested sarcopenia as a prognostic factor associated with poor survival and increased resistance and toxicity to chemotherapy in patients with various malignancies, including breast, small cell lung, urothelial, and gastric cancers (69-72). In ovarian cancer, conflicting results have been reported: while some studies concluded that sarcopenia adversely affected patients' PFS or OS (73, 74), others could not determine a significant association of sarcopenia with survival outcomes (75, 76). There were differences in study design, population, disease setting, and definition of sarcopenia among the studies; therefore, careful attention is required to interpret the study results. Moreover, considering the fact that body composition is different among the Organisation for Economic Co-operation and Development (OECD) member countries (77), sarcopenia and its impact on cancer prognosis may vary by geographical regions and ethnicities.

To determine sarcopenia, recent studies have suggested utilization of CT scans. A cross-sectional image of CT scans at the level of the third lumbar

vertebra (L3) is known to represent an individual's body composition, such as total body skeletal muscle and adipose tissues and fat distribution (78, 79). Moreover, CT scans are acquired routinely as part of cancer patients' care, so quantification of body composition using CT scans is quite possible.

To our knowledge, clinical significance of sarcopenia in Korean ovarian cancer patients has not been explored. Thus, we aimed to investigate impact of sarcopenia on survival outcomes in Korean patients with advanced-stage high-grade serous ovarian carcinoma (HGSOC), which is the predominant histologic type of ovarian cancer. In this study, sarcopenia was determined based on the pre-treatment CT scan; the fat composition was also measured considering the fact that the Asian population generally has a higher body fat percentage than the Western population at the same BMI (80).

2. Materials and Methods

2.1 Study population

From the Ovarian Cancer Cohort Database, we searched patients who met the following inclusion criteria: (1) patients older than 18 years of age, (2) those with HGSOC diagnosed and primarily treated at SNUH between January 2010 and December 2017, and (3) those with FIGO stage III-IV disease. However, patients with the following conditions were excluded: (1) patients with any malignancy other than HGSOC, (2) those with insufficient clinical data, (3) those who did not undergo pre-treatment CT scans, and (4) those who were underweight based on pre-treatment BMI (<18.5 kg/m^2). In total, 179 patients who met these criteria were included in this analysis.

2.2 CT image analysis and definition of sarcopenia

For the evaluation of sarcopenia, a cross-sectional area of the muscle at the level of L3 vertebral body was measured using baseline CT scans. Applying previously validated boundaries of -190 to -30 Hounsfield unit (HU) for fat tissue and -29 to 150 HU for skeletal muscle (81), an experienced radiologist (5 years of genitourinary imaging experience) who was blinded to the clinical outcome measured total abdominal muscle area (cm^2), intramuscular fat area (cm^2), visceral fat area (cm^2), and subcutaneous fat area (cm^2). This CT image analysis was conducted by semi-automatic technique using AsanJ-Morphometry software (Asan Image Metrics, Seoul, Korea) (**Figure 16A–C**).

Total abdominal muscle area (cm^2) was normalized for height (m^2) and reported as lumbar skeletal muscle index (SMI). To date, the sex-specific cutoff values of SMI for sarcopenia have not been validated in Korean healthy individuals. Adoption of the cutoff values suggested by Japanese study groups was deterred because they were developed in different study populations (e.g., patients with liver disease, (82)) or had age limitations (e.g., <50 years, (83)). In addition, proportions of populations with overweight-obesity are even different between Korea and Japan according to the OECD Health Statistics 2019 (77). Therefore, we defined sarcopenia as SMI of <39.0 cm^2/m^2 according to the proposed cutoff value by an international consensus, and divided patients into sarcopenia group (<39.0 cm^2/m^2) and no sarcopenia group (control group; ≥39.0 cm^2/m^2) (84). We also calculated other body composition indices, such as fat-to-muscle ratio (FMR), visceral-to-subcutaneous fat ratio (VSR), and

skeletal muscle mass-to-visceral fat ratio (SVR).

2.3 Data collection

We collected patients' clinicopathologic characteristics including age, co-morbidities such as hypertension or diabetes, American Society of Anesthesiologists score, FIGO stage, NAC, residual tumor size after PDS or IDS, and regimens and cycles of adjuvant chemotherapy. Patients treated with NAC received 3–4 cycles of taxane- and platinum-based chemotherapy before surgery, and optimal debulking surgery was considered when no gross residual tumor was achieved.

Patients' pre-treatment BMI was calculated as body weight (kg) divided by height squared (m^2), which were measured at the time of diagnosis. All patients were classified into three groups based on the following BMI criteria suggested by the World Health Organization for the Asian population: normal ($\geq$18.5 kg/m^2 and <23.0 kg/m^2), overweight ($\geq$23.0 kg/m^2 and <25.0 kg/m^2), and obese ($\geq$25.0 kg/m^2) (80).

Data acquisition also included serum CA-125 levels, hemoglobin, albumin, and differential blood cell counts including neutrophils, lymphocytes, monocytes, and platelets at initial diagnosis, less than a month prior to either PDS or the start date of NAC. As systemic inflammatory indices, we calculated the neutrophil-to-lymphocyte ratio (NLR), monocyte-to-lymphocyte ratio (MLR), and platelet-to-lymphocyte ratio (PLR). As a pre-treatment nutritional index, we calculated the prognostic nutritional index (PNI) as follows: 10 × serum albumin (g/dL) + 0.005 × peripheral blood lymphocyte count (/uL) (85).

In terms of survival data, OS was defined as the time interval between the date of diagnosis and the date of cancer-related death or the end of the study. During the surveillance, patients received CT scanning routinely every three to four months for the first two years, every six months for the next two years, and thereafter, every year or when symptoms or examination findings were suspicious for recurrence. Therefore, we defined PFS as the time interval between the start date of primary treatment and the date of image-confirmed disease progression, which was assessed based on the RECIST version 1.1 (60).

2.4 Statistical analysis

We compared the patients' clinicopathologic characteristics and survival outcomes between the sarcopenia and control groups. We used Student's t-test and the Mann-Whitney U test for comparisons of continuous variables and Pearson's chi-squared and Fisher's exact test for categorical variables. For survival analysis, we conducted the Kaplan-Meier methods with log-rank test. Multivariate analysis was performed using a Cox proportional-hazards model, and adjusted hazard ratios (aHRs) and 95% confidence intervals (CIs) were calculated. We used IBM SPSS Statistics software (version 25.0; SPSS Inc., Chicago, IL, USA) for these analyses. Correlation values were calculated by the Pearson's correlation coefficient test using the GraphPad Prism 5 software (GraphPad Inc., La Jolla, CA, USA). A P value <0.05 was considered statistically significant.

2.5 Ethical statement

This retrospective cohort study was approved by the Institutional Review Board of SNUH (No. H-1911-171-1082) which waived the requirement to obtain informed consent.

3. Results

3.1 Analysis in all patients

Patients' clinicopathologic characteristics are presented in **Table 6.** The sarcopenia group (n=76) had significantly lower pre-treatment BMI (mean, 22.1 vs. 24.7 kg/m^2; *P* <0.001) and received NAC less frequently (17.1% vs. 30.1%; *P*=0.046), compared to the control group (n=103). Other characteristics showed no significant difference between two groups. The patients' initial body composition and laboratory results are presented in **Table 7**. The sarcopenia group showed less skeletal muscle area (median, 88.1 vs. 106.1 cm^2; *P* <0.001) and total fat area (median, 188.5 vs. 230.7 cm^2; *P* <0.001). Among the various calculated body composition indices, all others except SMI were similar between the sarcopenia and control groups. There were no differences in the laboratory results, inflammatory indices, and nutritional index between the groups.

The median length of observation was 42.7 months, and it was not different between both groups (45.9 vs. 41.5 months; *P*=0.497). During this period, 140 patients (78.2%) experienced disease recurrence, and 57 patients (31.8%) died of disease. Patients in the sarcopenia and control groups showed similar PFS (median, 18.3 vs. 18.7 months; *P*=0.450; **Figure 17A**) and OS (5-year survival

rate, 64.1% vs. 59.3%; *P*=0.287; **Figure 17B**).

Multivariate analyses adjusting patients' age, FIGO stage, serum CA-125 levels, primary treatment strategy, residual tumor size after surgery, and BMI revealed that pre-treatment sarcopenia status did not influence patients' PFS and OS (**Table 8**). Instead, age ≥58 years (aHR, 1.458; 95% CI, 1.024–2.077; *P*=0.037) and gross residual tumor (aHR, 1.504; 95% CI, 1.068–2.119; *P*=0.020) were identified as independent poor prognostic factors for PFS. For OS, NAC rather than PDS (aHR, 2.000; 95% CI, 1.096–3.649; *P*=0.024) and gross residual tumor (aHR, 2.142; 95% CI, 1.258–3.647; *P*=0.005) were the poor prognostic factors.

3.2 Subgroup analysis in sarcopenia patients

Because we focused on patients' relative fat mass, we adopted FMR among the calculated body composition indices. As the median FMR of all patients was 2.1, we subdivided the patients into FMR low (<2.1) and high (≥2.1) groups. Among the patients without sarcopenia (n=103), no differences in PFS and OS were observed between the FMR low and high groups (*P*=0.453 and *P*=0.975, respectively) (**Figure 18A,B**).

Next, we performed subgroup analysis confined to the sarcopenia group (n=76). Patients' clinicopathologic characteristics are presented in **Table 9**. Compared to patients with low FMR, patients with high FMR were significantly older (mean, 60.1 vs. 54.0 years; *P*=0.006), and had higher pre-treatment BMI (mean, 23.6 vs. 20.7 kg/m^2; *P* <0.001) and prevalence of dyslipidemia (15.8% vs. 0%; *P*=0.025). Other characteristics were similar

between the FMR high and low groups. Sarcopenia patients' initial body composition and laboratory results are presented in **Table 10**. Compared to the FMR low group, the FMR high group showed higher total fat area (median, 228.1 vs. 141.5 cm^2; *P* <0.001) and VSR (median, 0.6 vs. 0.3; *P*=0.001), and lower SVR) median, 1.1 vs. 2.5; *P* <0.001). However, skeletal muscle area as well as SMI were similar between both groups. There were no differences in the laboratory results, inflammatory indices, and nutritional index between the two groups.

In the sarcopenia group, patients with FMR showed significantly worse OS than those with low FMR (5-year survival rate, 44.7% vs. 80.0%; *P*=0.046), whereas PFS was not different (*P*=0.365) (**Figure 18C,D**). Multivariate analyses identified high FMR as an independent poor prognostic factor for OS in this group (aHR, 3.377; 95% CI, 1.170–9.752; *P*=0.024), whereas high FMR did not influence patients' PFS (*P*=0.825) (**Table 11**). Other poor prognostic factors for OS were NAC rather than PDS (aHR, 3.310; 95% CI, 1.096–10.000; *P*=0.034) and gross residual tumor after surgery (aHR, 4.377; 95% CI, 1.655–11.578; *P*=0.003).

3.3 Correlations between body composition and systemic inflammatory indices

We investigated the correlations between SMI and the three systemic inflammatory indices, NLR, MLR, and PLR. While SMI was significantly associated with BMI (Pearson's correlation coefficient *r*=0.478; *P* <0.001), there were no correlations between SMI and either NLR, MLR, or PLR (**Figure**

19A–D).

To elucidate the underlying mechanisms of high FMR and poor survival outcome in sarcopenia patients, correlations between FMR and the three systemic inflammatory indices—NLR, MLR, and PLR—were also investigated. While FMR was significantly associated with BMI (Pearson's correlation coefficient r=0.778; P <0.001), significant correlations were not observed between FMR and NLR, between FMR and MLR, and between FMR and PLR (**Figure 19E–H**).

4. Discussion

In this study, we investigated the impact of pre-treatment sarcopenia on survival outcomes in patients with advanced-stage HGSOC and revealed that there was no significant association between sarcopenia and recurrence rate or survival. However, further subgroup analysis identified high FMR as a poor prognostic factor for OS in sarcopenia patients.

Unlike other malignancies in which sarcopenia is associated with decreased OS and increased post-operative morbidity (86, 87), inconsistent results on the relationship between sarcopenia and survival outcome are observed among the studies regarding ovarian cancer. There are two representative retrospective studies: while Bronger et al. reported the baseline sarcopenia is an independent poor prognostic factor for PFS and OS in advanced-stage serous ovarian cancer (74), Rutten et al. demonstrated that sarcopenia was not a prognostic factor for OS or major complications in ovarian cancer patients undergoing PDS (75). Most studies were conducted in Western populations whose body composition

is different from that of Asians. Recently, a Japanese retrospective study showed results similar to those of our study; pre-treatment SMI was not associated with ovarian cancer patients' PFS and OS (88). However, that study included early-stage disease and histologic types other than HGSOC, which is definitely different compared to our study.

To date, researches on sarcopenia in cancer patients have been conducted in the context of cancer cachexia. Patients with HGSOC are at high risk of sarcopenia and cachexia. First, as the disease is often detected in a much-progressed state, the patients might already have cachexia at the time of diagnosis. Second, an enlarging tumor mass induces metabolic dysfunction towards catabolism, while bowel obstructions during disease progression cause anorexia or reduced food intake (89). Third, newly diagnosed patients undergo aggressive cytoreductive surgery followed by taxane- and platinum-based chemotherapy as an established standard of care, which further aggravate anorexia and loss of body weight (47). Consequently, poor nutritional status and loss of muscle mass and strength is highly expected in patients with ovarian cancer. Previously, our research team reported that underweight status, one of the representative features of cachexia, was a poor prognostic factor in patients with advanced-stage ovarian cancer (90). In the current study, rather than cancer cachexia, we focused on sarcopenia itself which may be incidentally discovered at the time of diagnosis of ovarian cancer. For this purpose, we excluded pre-treatment underweight patients in whom cancer cachexia could already be dominant.

CT scans are known to distinguish fat and muscle tissue accurately with high

reproducibility by using specific attenuation of each tissue (91). The most commonly used and validated HU range for adipose tissue is -190 to -30. However, there is an inconsistency between the literature with the HU range for muscle tissue, which starts from either 0 or -29 and ends at 100 or 150. Exclusion of the area ranging from -29 to 0 HU may result in significant loss of the total muscle area. Instead, we used -29 to 150 HU for muscle tissue so as not to miss the low attenuation muscle, same as that used in previous studies (92, 93).

Although there was no statistical difference in PFS and OS between the sarcopenia and control groups, we found that high FMR is an independent prognostic factor for OS in the sarcopenia group. The coexistence of sarcopenia and obesity (sarcopenic obesity) seems to affect patients' survival outcomes equal to or greater than the sum of the respective risks of obesity and sarcopenia alone (94). A previous study has reported that the presence of sarcopenic obesity increased patients' mortality in colorectal cancer (95). In the current study, we focused on amount of the fat relative to the muscle, rather than BMI, considering the fact that Asians have a higher body fat percentage than Westerners at the same BMI (80), and similar results were found with the previous studies.

One remarkable observation in the current study is that we tried to elucidate the mechanisms underlying the relationship between high FMR and decreased survival in sarcopenic patients with advanced-stage HGSOC. Previously, our research team reported that adipose stem cells from visceral and subcutaneous fat facilitated the growth and migration of ovarian cancer cells via IL-

6/JAK2/STAT3 pathway (96). Adding to this, other researchers have reported that visceral obesity is associated with a chronic inflammatory state, which leads to adverse metabolic consequences (97). The relationship between sarcopenia and systemic inflammation has been also reported (98). In this context, we hypothesized that systemic inflammatory indices (NLR, MLR, and PLR) would be different between the high and low FMR groups. However, there were no differences between both groups, and correlations were not observed between FMR and the three systemic inflammatory indices. Similar correlations were also observed between SMI and the inflammatory indices. These findings might be related to the small sample size or exclusion of underweight patients. Moreover, investigation of other systemic inflammatory markers and adipose tissue-derived cytokines, such as leptin, IL-6 and TNF-α, may answer our hypothesis exactly.

In keeping with the era of precision medicine, early identification of adverse body composition which might influence patients' survival outcome would be one of the important issues. For patients who have high FMR, aerobic exercises may be recommended to reduce adipose tissue. To date, intervention studies to prevent sarcopenia or maintain skeletal muscle mass in patients with ovarian cancer is still insufficient. Nevertheless, as recommended by various societies, prescription of resistance-type exercise training and a protein-rich diet or protein supplement should be also considered for HGSOC patients with sarcopenia. Hormone replacement therapy or vitamin D may be given, but more evidence is needed (99-101). For those who have chemotherapy-induced nausea and vomiting, adequate anti-emetics as well as parenteral nutrition

should be provided. If patients suffer from dyspepsia or abdominal distention owing to large amount of ascites, drainage of ascitic fluid may improve patients' symptoms as well as nutritional status. If there is long persistent seeding ileus, procedures such as stoma formation may be considered as well. Prior to administering these interventions, all HGSOC patients should be screened for sarcopenia and adiposity at the time of diagnosis. As pre-treatment or baseline CT scans are commonly performed to determine the severity of disease and to establish a treatment plan in most patients, routine screening for body composition would be available and practical.

The current study has several limitations. First, a small sample size with possible selection bias that originates from the retrospective study design might be problematic. Second, the sequential change of body composition in each individual was not considered. Third, associations between sarcopenia and surgery or chemotherapy-related complications were not investigated. Finally, although muscle mass was successfully measured by using CT scans, muscle quality was hard to know by this imaging modality. Decreased muscle quality is known to be associated with the fatty degeneration or fatty infiltration of the muscle (i.e., myosteatosis). Currently, MRI is the best modality to evaluate the muscle quality and myosteatosis. In addition, MRI may also provide information on inflammation, edema, fibrosis, and atrophy in the muscle (102-104).

However, because of its high cost, limited availability, and long image acquisition time, MRI-based body composition assessment is not a routine clinical practice. Most of our study population did not undergo pre-treatment

MRI, so accurate assessment of muscle quality was unavailable. Despite this study's limitations, the current study is the first study to adopt CT-based body composition measurement techniques to identify prognostic factors in Korean ovarian cancer patients.

In conclusion, we investigated the clinical significance of sarcopenia in Korean patients with advanced-stage HGSOC and found that sarcopenia did not influence patients' recurrence rates and survival. However, among the sarcopenia patients, those who had relatively high levels of fat compared to muscle mass showed worse OS. Further translational researches and prospective studies are warranted.

Table 6. Patients' clinicopathologic characteristics

Characteristics	All (n=179, %)	No Sarcopenia (n=103, %)	Sarcopenia (n=76, %)	*P*
Age, years				
Mean ± SD	57.5 ± 10.6	57.8 ± 11.1	57.0 ± 9.9	0.615
BMI*, kg/m^2				
Mean ± SD	23.6 ± 3.2	24.7 ± 3·3	22.1 ± 2.3	<0.001
Normal (18.5–22.9)	81 (45.3)	35 (34.0)	46 (60.5)	<0.001
Overweight (23.0–24.9)	52 (29.1)	30 (29.1)	22 (28.9)	
Obesity (≥25.0)	46 (25.7)	38 (36.9)	8 (10.5)	
Comorbidities				
Hypertension	48 (26.8)	28 (27.2)	20 (26.3)	0.897
Diabetes	15 (8.4)	10 (9.7)	5 (6.6)	0.455
Dyslipidemia	21 (11.7)	15 (14.6)	6 (7.9)	0.171
ASA score				0.080
1	63 (35.2)	31 (30.1)	32 (42.1)	
2	104 (58.1)	67 (65.0)	37 (48.7)	
3	12 (6.7)	5 (4.9)	7 (9.2)	
FIGO stage				0.653
IIIA1	8 (4.5)	5 (4.9)	3 (3.9)	
IIIA2	6 (3.4)	4 (3.9)	2 (2.6)	
IIIB	17 (9.5)	9 (8.7)	8 (10.5)	
IIIC	91 (50.8)	50 (48.5)	41 (53.9)	
IVA	10 (5.6)	4 (3.9)	6 (7.9)	
IVB	47 (26.3)	31 (30.1)	16 (21.1)	
CA-125, IU/ml				
Median (range)	801.0 (5.1–24720)	833.0 (7–10000)	793.0 (5.1–24720)	0.829
Primary treatment strategy				0.046
PDS	135 (75.4)	72 (69.9)	63 (82.9)	
NAC	44 (24.6)	31 (30.1)	13 (17.1)	
Residual tumor after PDS/IDS				0.336
No gross	114 (63.7)	67 (65.0)	47 (61.8)	
<1 cm	44 (24.6)	26 (25.2)	18 (23.7)	
1–2 cm	10 (5.6)	3 (2.9)	7 (9.2)	
≥2 cm	11 (6.1)	7 (6.8)	4 (5.3)	
Regimen of first-line chemotherapy				0.368
Paclitaxel-Carboplatin	161 (89.9)	93 (90.3)	68 (89.5)	0.393
Docetaxel-Carboplatin	14 (7.8)	9 (8.7)	5 (6.6)	
Paclitaxel-Carboplatin-Bevacizumab	4 (2.2)	1 (1.0)	3 (3.9)	
Main cycles of first-line chemotherapy				
Median (range)	6 (4–12)	6 (4–12)	6 (4–12)	0.438
4–6	123 (68.7)	70 (68.0)	53 (69.7)	
7–9	50 (27.9)	31 (30.1)	19 (25.0)	
10–12	6 (3.4)	2 (1.9)	4 (5.3)	
Recurrence	140 (78.2)	78 (75.7)	62 (81.6)	0.349
PSR†	95 (53.1)	47 (45.6)	48 (63.2)	0.031
PRR	45 (25.1)	31 (30.1)	14 (18.4)	
Platinum sensitivity				0.075
Platinum-sensitive‡	134 (74.9)	72 (69.9)	62 (81.6)	
Platinum-resistant	45 (25.1)	31 (30.1)	14 (18.4)	

Abbreviations: ASA, American Society of Anesthesiologists; BMI, body mass index; CA-125, cancer antigen 125; FIGO, International Federation of Gynecology and Obstetrics; IDS, interval debulking surgery; NAC, neoadjuvant chemotherapy; PDS, primary debulking surgery; PRR,

platinum-resistant recurrence; PSR, platinum-sensitive recurrence; SD, standard deviation.

*In this study, underweight patients (BMI <18.5 kg/m^2) were excluded in analysis.

†PSR was defined as relapse ≥6 months after completion of taxane- and platinum-based chemotherapy, whereas PRR as relapse <6 months.

‡In addition to PSR, the patients who completed taxane- and platinum-based chemotherapy and did not experience disease recurrence during at least 6 months of follow-up period were considered platinum-sensitive.

Table 7. Body composition and laboratory results of all patients

Characteristics	All (n=179, %)	No Sarcopenia (n=103, %)	Sarcopenia (n=76, %)	*P*
Body composition at diagnosis*				
Skeletal muscle area, cm^2	98.0 (64.1–209.8)	106.1 (84.8–209.8)	88.1 (64.1–109.0)	<0.001
Total fat area, cm^2	211.8 (42.2–612.5)	230.7 (78.8–612.5)	188.5 (42.2–458.2)	<0.001
Subcutaneous fat	131.7 (34.4–310.8)	154.0 (55.8–310.8)	119.8 (34.4–252.0)	<0.001
Visceral fat	70.4 (6.6–289.4)	81.5 (11.2–289.4)	59.6 (6.6–213.0)	0.001
Muscle fat	6.2 (0.7–36.2)	6.5 (0.7–36.2)	5.3 (1.2–31.6)	0.103
Calculated body composition index*				
Skeletal muscle index (SMI), cm^2/m^2	40.3 (27.1–79.2)	42.6 (39.0–79.2)	36.3 (27.1–39.0)	<0.001
Fat-to-muscle ratio (FMR)	2.1 (0.5–6.5)	2.1 (0.8–6.5)	2.1 (0.5–4.9)	0.508
Visceral-to-subcutaneous fat ratio (VSR)	0.5 (0.1–2.9)	0.5 (0.1–1.4)	0.4 (0.1–2.9)	0.212
Skeletal muscle mass-to-visceral fat ratio (SVR)	1.4 (0.3–14.2)	1.3 (0.3–8.7)	1.5 (0.5–14.2)	0.178
Laboratory test at diagnosis*				
Hemoglobin, g/dL	12.2 (8.3–14.9)	12.2 (9.1–14.9)	12.4 (8.3–14.6)	0.491
WBC count, 10^3/uL	7.0 (1.5–17.0)	6.9 (1.5–14.7)	7.1 (3.5–17.0)	0.417
Neutrophil (%)	68.9 (28.0–92.0)	68.9 (28.0–92.0)	68.9 (47.0–83.0)	0.734
Lymphocyte (%)	21.7 (5.0–57.0)	22.2 (5.0–57.0)	21.2 (9.4–42.9)	0.772
Monocyte (%)	6.8 (0.7–20.9)	6.8 (0.7–20.9)	6.9 (3.7–16.0)	0.335
Platelet count, 10^3/uL	316.5 (95.0–698.0)	312.0 (95.0–698.0)	323.0 (159.0–634.0)	0.355
Albumin, g/dL	3.9 (2.3–5.1)	3.8 (2.3–4.6)	4.0 (2.4–5.1)	0.128
Calculated inflammatory index*				
Neutrophil-to-lymphocyte ratio (NLR)	3.2 (0.5–18.4)	3.1 (0.5–18.4)	3.2 (1.2–8.8)	0.945
Monocyte-to-lymphocyte ratio (MLR)	0.3 (0.1–0.9)	0.3 (0.1–0.9)	0.3 (0.1–0.9)	0.378
Platelet-to-lymphocyte ratio (PLR)	204.9 (71.6–768.5)	208.3 (71.6–768.5)	204.7 (77.2–628.1)	0.923
Calculated nutritional index				
Prognostic nutritional index (PNI)				
Mean ± SD	46.0 ± 7.0	45.3 ± 7.0	47.0 ± 6.9	0.100

*Median (range). Abbreviations: SD, standard deviation; WBC, white blood cell.

Table 8. Factors associated with patients' survival outcomes

Characteristics	(A) Progression-Free Survival						(B) Overall Survival					
	Univariate Analysis			Multivariate Analysis			Univariate Analysis			Multivariate Analysis		
	HR	95% CI	*P*	aHR	95% CI	*P*	HR	95% CI	*P*	aHR	95% CI	*P*
Age, years												
<58	1	–	–	1	–	–	1	–	–	1	–	–
≥58	1.558	1.116–2.175	0.009	1.458	1.024–2.077	0.037	1.551	0.919–2.618	0.101	1.213	0.692–2.127	0.500
FIGO stage												
III	1	–	–	1	–	–	1	–	–	1	–	–
IV	1.342	0.944–1.908	0.101	1.216	0.820–1.805	0.330	1.490	0.861–2.579	0.154	1.256	0.690–2.288	0.456
CA-125, IU/ml												
<800	1	–	–	1	–	–	1	–	–	1	–	–
≥800	1.164	0.835–1.622	0.370	1.140	0.811–1.602	0.451	1.110	0.660–1.867	0.695	0.964	0.560–1.660	0.894
Primary treatment strategy												
PDS	1	–	–	1	–	–	1	–	–	1	–	–
NAC	1.669	1.151–2.419	0.007	1.380	0.902–2.113	0.138	2.376	1.392–4.057	0.002	2.000	1.096–3.649	0.024
Residual tumor after PDS/IDS												
No gross	1	–	–	1	–	–	1	–	–	1	–	–
Gross	1.568	1.119–2.198	0.009	1.504	1.068–2.119	0.020	2.169	1.286–3.658	0.004	2.142	1.258–3.647	0.005
BMI, kg/m^2												
Normal (18.5–22.9)	1	–	–	1	–	–	1	–	–	1	–	–
Overweight (23.0–24.9)	0679	0.449–1.029	0.068	0.656	0.429–1.004	0.052	0.728	0.366–1.450	0.367	0.707	0.347–1.437	0.338
Obesity (≥25.0)	1.184	0.799–1.755	0.399	1.132	0.742–1.726	0.564	1.638	0.909–2.951	0.100	1.261	0.661–2.405	0.481
Sarcopenia												
No	1	–	–	1	–	–	1	–	–	1	–	–
Yes	0.879	0629–1.228	0.451	1.292	0.906–1.843	0.157	0.747	0.436–1.280	0.289	0.870	0.488–1.550	0.636

Abbreviations: aHR, adjusted hazard ratio; BMI, body mass index; CA-125, cancer antigen 125; CI, confidence interval; FIGO, International Federation of Gynecology and Obstetrics; HR, hazard ratio; IDS, interval debulking surgery; NAC, neoadjuvant chemotherapy; PDS, primary debulking surgery.

Table 9. Clinicopathologic characteristics of sarcopenia patients

Characteristics	FMR Low (n=38, %)	FMR High (n=38, %)	*P*
Age, years			
Mean ± SD	54.0 ± 8.2	60.1 ± 10.6	0.006
BMI*, kg/m^2			
Mean ± SD	20.7 ± 1.5	23.6 ± 1.9	<0.001
Normal (18.5–22.9)	33 (86.8)	13 (34.2)	<0.001
Overweight (23.0–24.9)	5 (13.2)	17 (44.7)	
Obesity (≥25.0)	0	8 (21.1)	
Comorbidities			
Hypertension	7 (18.4)	13 (34.2)	0.118
Diabetes	3 (7.9)	2 (5.3)	>0.999
Dyslipidemia	0	6 (15.8)	0.025
ASA score			0.466
1	16 (42.1)	16 (42.1)	
2	20 (52.6)	17 (44.7)	
3	2 (5.3)	5 (13.2)	
FIGO stage			0.613
III	28 (73.7)	26 (68.4)	
IV	10 (26.3)	12 (31.6)	
CA-125, IU/ml			
Median (range)	793.0 (13–24720)	712.5 (5.1–7821)	0.949
Primary treatment strategy			0.361
PDS	33 (86.8)	30 (78.9)	
NAC	5 (13.2)	8 (21.1)	
Residual tumor after PDS/IDS			0.533
No gross	23 (60.5)	24 (63.2)	
<1 cm	11 (28.9)	7 (18.4)	
1–2 cm	2 (5.3)	5 (13.2)	
≥2 cm	2 (5.3)	2 (5.3)	
Regimen of first-line chemotherapy			0.306
Paclitaxel-Carboplatin	36 (94.7)	32 (84.2)	
Docetaxel-Carboplatin	1 (2.6)	4 (10.5)	
Paclitaxel-Carboplatin-Bevacizumab	1 (2.6)	2 (5.3)	
Main cycles of first-line chemotherapy			
Median (range)	6 (4–12)	6 (4–12)	0.374
4–6	28 (73.7)	25 (65.8)	0.725
7–9	8 (21.1)	11 (28.9)	
10–12	2 (5.3)	2 (5.3)	
Recurrence	30 (78.9)	32 (842)	0.554
PSR†	24 (63.2)	24 (63.2)	0.638
PRR	6 (15.8)	8 (21.1)	
Platinum sensitivity			0.554
Platinum-sensitive‡	32 (84.2)	30 (78.9)	
Platinum-resistant	6 (15.8)	8 (21.1)	

Abbreviations: ASA, American Society of Anesthesiologists; BMI, body mass index; CA-125, cancer antigen 125; FIGO, International Federation of Gynecology and Obstetrics; IDS, interval debulking surgery; NAC, neoadjuvant chemotherapy; PDS, primary debulking surgery; PRR, platinum-resistant recurrence; PSR, platinum-sensitive recurrence; SD, standard deviation.

*In this study, underweight patients (BMI <18.5 kg/m^2) were excluded in analysis.

†PSR was defined as relapse ≥6 months after completion of taxane- and platinum-based chemotherapy, whereas PRR as relapse <6 months.

‡In addition to PSR, the patients who completed taxane- and platinum-based chemotherapy and did not experience disease recurrence during at least 6 months of follow-up period were considered platinum-sensitive.

Table 10. Body composition and laboratory results of sarcopenia patients

Characteristics	FMR Low (n=38, %)	FMR High (n=38, %)	*P*
Body composition at diagnosis*			
Skeletal muscle area, cm^2	89.8 (74.5–109.0)	86.4 (64.1–104.8)	0.094
Total fat area, cm^2	141.5 (42.2–199.3)	228.1 (166.0–458.2)	<0.001
Subcutaneous fat	97.1 (34.4–165.4)	138.3 (54.6–252.0)	<0.001
Visceral fat	35.2 (6.6–79.4)	82.1 (30.1–213.0)	<0.001
Muscle fat	3.8 (1.2–15.2)	7.8 (2.3–31.6)	<0.001
Calculated body composition index*			
Skeletal muscle index (SMI), cm^2/m^2	36.0 (27.1–39.0)	37.4 (28.7–39.0)	0.228
Fat-to-muscle ratio (FMR)	1.6 (0.5–2.1)	2.6 (2.1–4.8)	<0.001
Visceral-to-subcutaneous fat ratio (VSR)	0.3 (0.1–1.3)	0.6 (0.2–2.9)	0.001
Skeletal muscle mass-to-visceral fat ratio (SVR)	2.5 (1.0–14.2)	1.1 (0.5–2.6)	<0.001
Laboratory test at diagnosis*			
Hemoglobin, g/dL	12.1 (8.3–14.6)	12.5 (9.2–14.3)	0.569
WBC count, 10^3/uL	7.4 (3.5–15.3)	6.9 (4.1–17.0)	0.971
Neutrophil (%)	69.7 (47.0–83.0)	68.4 (49.7–81.2)	0.646
Lymphocyte (%)	21.5 (9.4–37.0)	21.2 (9.7–42.9)	0.893
Monocyte (%)	7.2 (3.7–16.0)	6.5 (4.5–13.5)	0.557
Platelet count, 10^3/uL	323.5 (159.0–634.0)	3225 (202.0–564.0)	0.383
Albumin, g/dL	3.9 (2.8–5.0)	4.0 (2.4–5.1)	0.521
Calculated inflammatory index*			
Neutrophil-to-lymphocyte ratio (NLR)	3.2 (1.4–8.8)	3.3 (1.2–8.4)	0.884
Monocyte-to-lymphocyte ratio (MLR)	0.3 (0.1–0.8)	0.3 (0.1–0.9)	0.771
Platelet-to-lymphocyte ratio (PLR)	201.0 (77.2–547.0)	211.2 (97.3–682.1)	0.633
Calculated nutritional index			
Prognostic nutritional index (PNI)			
Mean ± SD	46.7 (34.5–59.1)	48.2 (27.7–64.0)	0.357

*Median (range). Abbreviations: SD, standard deviation; WBC, white blood cell.

Table 11. Factors associated with sarcopenia patients' survival outcomes

Characteristics	(A) Progression-Free Survival						(B) Overall Survival					
	Univariate Analysis			Multivariate Analysis			Univariate Analysis			Multivariate Analysis		
	HR	95% CI	*P*	aHR	95% CI	*P*	HR	95% CI	*P*	aHR	95% CI	*P*
Age, years												
<58	1	–	–	1	–	–	1	–	–	1	–	–
≥58	1.934	1.158–3.229	0.012	1.905	1.065–3.407	0.030	1.593	0.669–3.795	0.293	1.041	0.417–2.598	0.932
FIGO stage												
III	1	–	–	1	–	–	1	–	–	1	–	–
IV	1.063	0.612–1.845	0.829	0.917	0.484–1.739	0.791	1.394	0.557–3.488	0.487	0.947	0.345–2.594	0.915
CA-125, IU/ml												
<800	1	–	–	1	–	–	1	–	–	1	–	–
≥800	0.933	0.563–1.546	0.787	0.863	0.492–1.514	0.608	0.999	0.424–2.354	0.998	1.171	0.414–3.314	0.766
Primary treatment strategy												
PDS	1	–	–	1	–	–	1	–	–	1	–	–
NAC	1.456	0.773–2.742	0.245	1.254	0.594–2.644	0.553	2.933	1.177–7.309	0.021	3.310	1.096–10.000	0.034
Residual tumor after PDS/IDS												
No gross	1	–	–	1	–	–	1	–	–	1	–	–
Gross	2.274	1.363–3.795	0.002	2.270	1.334–3.861	0.003	3.587	1.442–8.922	0.006	4.377	1.655–11.578	0.003
BMI, kg/m^2												
Normal (18.5–22.9)	1	–	–	1	–	–	1	–	–	1	–	–
Overweight (23.0–24.9)	0.921	0.517–1.641	0.780	0.846	0.440–1.624	0.615	1.024	0.383–2.740	0.962	0.783	0.244–2.517	0.682
Obesity (≥25.0)	1.407	0.648–3.051	0.388	0.937	0.370–2.376	0.892	1.726	0.482–6.178	0.401	0.356	0.065–1.935	0.232
Fat-to-muscle ratio (FMR)												
<2.1	1	–	–	1	–	–	1	–	–	1	–	–
≥2.1	1.262	0.762–2.092	0.366	1.073	0.576–1.999	0.825	2.476	0.989–6.199	0.053	3.377	1.170–9.752	0.024

Abbreviations: aHR, adjusted hazard ratio; BMI, body mass index; CA-125, cancer antigen 125; CI, confidence interval; FIGO, International Federation of Gynecology and Obstetrics; HR, hazard ratio; IDS, interval debulking surgery; NAC, neoadjuvant chemotherapy; PDS, primary debulking surgery.

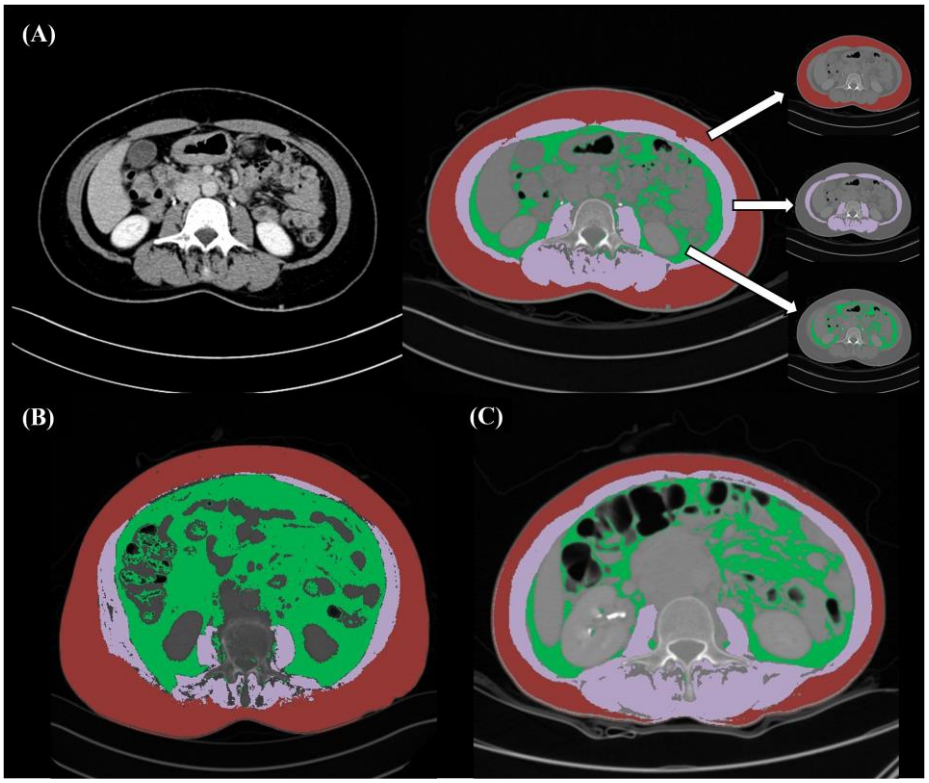

Figure 16. Evaluation of body composition using CT image. Preoperative axial CT image at the level of L3 vertebral body level. (A) A 52-year old woman with newly diagnosed high-grade serous ovarian carcinoma. Total abdominal muscle area (purple), visceral fat area (green), and subcutaneous fat area (red) are segmented by the semi-automatic technique; (B) A 73-year old woman with sarcopenia and high fat-to-muscle ratio (4.6); (C) A 53-year old woman with sarcopenia and low fat-to-muscle ratio (1.5).

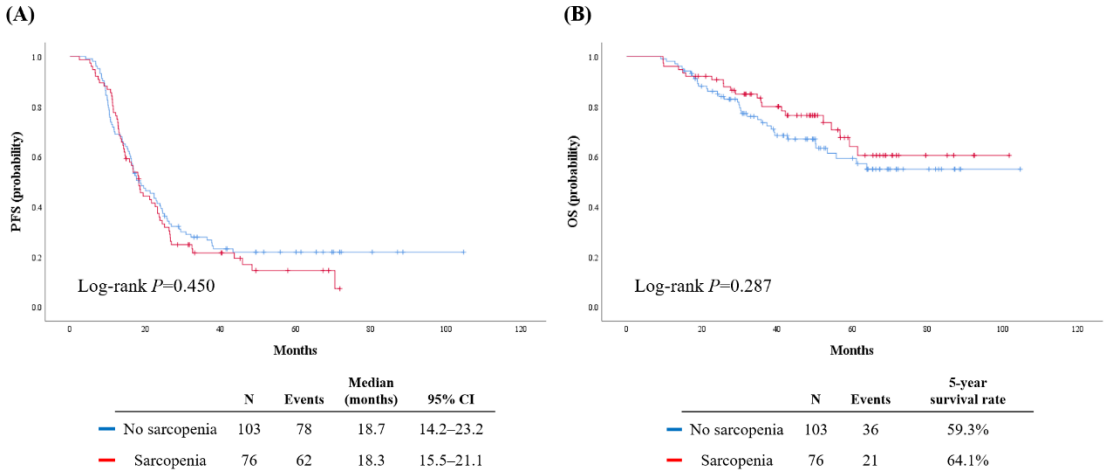

	N	Events	Median (months)	95% CI
No sarcopenia	103	78	18.7	14.2–23.2
Sarcopenia	76	62	18.3	15.5–21.1

	N	Events	5-year survival rate
No sarcopenia	103	36	59.3%
Sarcopenia	76	21	64.1%

Figure 17. Survival outcomes of patients. (A) Progression-free survival. (B) Overall survival.

Control group

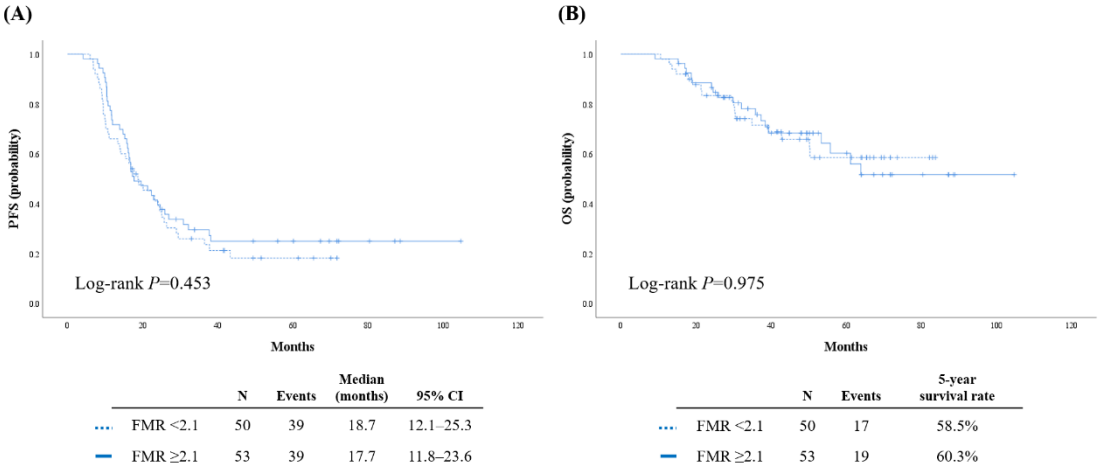

	N	Events	Median (months)	95% CI
FMR <2.1	50	39	18.7	12.1–25.3
FMR ≥2.1	53	39	17.7	11.8–23.6

	N	Events	5-year survival rate
FMR <2.1	50	17	58.5%
FMR ≥2.1	53	19	60.3%

Sarcopenia group

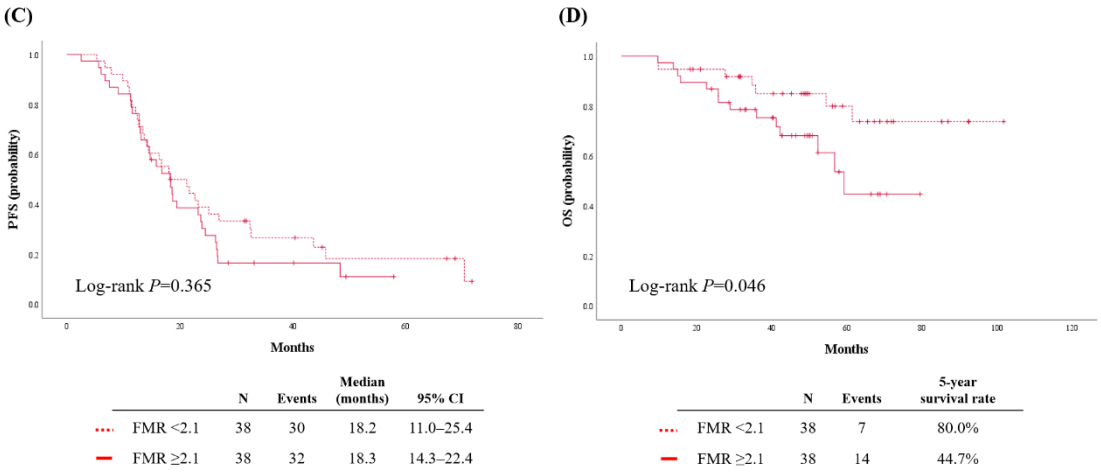

	N	Events	Median (months)	95% CI
FMR <2.1	38	30	18.2	11.0–25.4
FMR ≥2.1	38	32	18.3	14.3–22.4

	N	Events	5-year survival rate
FMR <2.1	38	7	80.0%
FMR ≥2.1	38	14	44.7%

Figure 18. Survival outcomes of patients by fat-to-muscle ratio. (Upper) Control group; (Lower) Sarcopenia group. (A,C) Progression-free survival; (B,D) Overall survival.

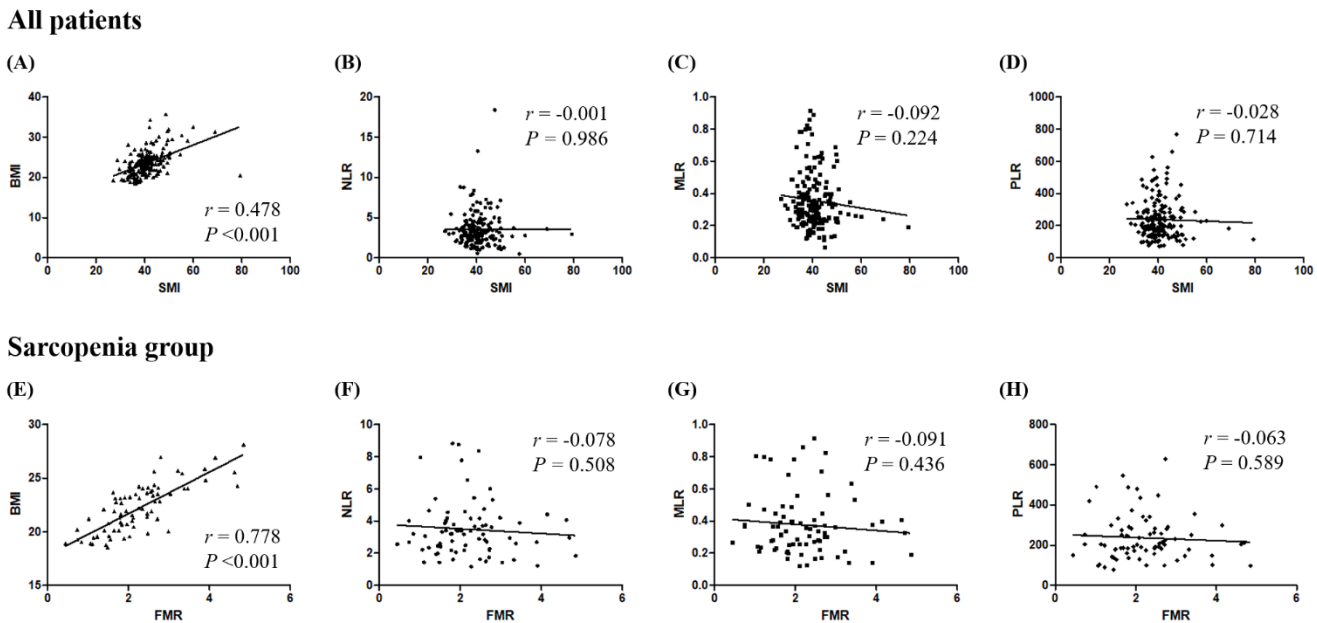

Figure 19. Correlations between body composition and systemic inflammatory indices. (Upper) Analyses according to skeletal muscle index in all patients; (Lower) Analyses according to fat to muscle ratio in sarcopenia patients. (A,E) Body mass index; (B,F) Neutrophil-to-lymphocyte ratio; (C,G) Monocyte-to-lymphocyte ratio; (D,H) Platelet-to-lymphocyte ratio.

Appendix

Appendix – List of publications related to this thesis

1. Kim SI, Kang N, Leem S, Yang J, Jo H, Lee M, et al. Metagenomic Analysis of Serum Microbe-Derived Extracellular Vesicles and Diagnostic Models to Differentiate Ovarian Cancer and Benign Ovarian Tumor. Cancers (Basel). 2020;12(5):1309. doi: 10.3390/cancers12051309. PMID: 32455705.
.

2. Kim SI, Song M, Hwangbo S, Lee S, Cho U, Kim JH, et al. Development of Web-Based Nomograms to Predict Treatment Response and Prognosis of Epithelial Ovarian Cancer. Cancer Res Treat. 2019;51(3):1144-55. doi: 10.4143/crt.2018.508. PMID: 30453728.

3. Kim SI, Kim TM, Lee M, Kim HS, Chung HH, Cho JY, et al. Impact of CT-Determined Sarcopenia and Body Composition on Survival Outcome in Patients with Advanced-Stage High-Grade Serous Ovarian Carcinoma. Cancers (Basel). 2020;12(3):559. doi: 10.3390/cancers12030559. PMID: 32121099.

Acknowledgements

I would like to express my sincere appreciation to a number of individuals who have supported my research in many ways. Without them, I would not have been able to complete my PhD study.

First of all, from the bottom of my heart I would like to thank my supervisor Professor Yong Sang Song for his consistent guidance and mentorship provided during my PhD study. I was lucky that I met him as a mentor that with his guidance and overall insight, I could grow both academically and personally.

I also would like to thank all the faculty members of Department of Obstetrics and Gynecology, Seoul National University Hospital who have taught and guided me into a wide-range of subjects in biomedical researches so that I could broaden my scopes of academic researches. I also would like to express my big thanks to all the collaborators who helped me throughout my study.

Also, I am extremely thankful to my colleagues, both current and past lab members at the lab of gynecologic oncology.

Finally, I wish to express my deepest gratitude to my family and friends who were always supportive spiritually and putting up with me during the compilation of this dissertation and my life in general.

References

1. Bray F, Ferlay J, Soerjomataram I, Siegel RL, Torre LA, Jemal A. Global cancer statistics 2018: GLOBOCAN estimates of incidence and mortality worldwide for 36 cancers in 185 countries. CA Cancer J Cin. 2018;68(6):394-424.
2. Siegel RL, Miller KD, Jemal A. Cancer statistics, 2019. CA Cancer J Clin. 2019;69(1):7-34.
3. Lim MC, Won YJ, Ko MJ, Kim M, Shim SH, Suh DH, et al. Incidence of cervical, endometrial, and ovarian cancer in Korea during 1999-2015. J Gynecol Oncol. 2019;30(1):e38.
4. Baldwin LA, Huang B, Miller RW, Tucker T, Goodrich ST, Podzielinski I, et al. Ten-year relative survival for epithelial ovarian cancer. Obstet Gynecol. 2012;120(3):612-8.
5. Myers ER, Bastian LA, Havrilesky LJ, Kulasingam SL, Terplan MS, Cline KE, et al. Management of adnexal mass. Evid Rep Technol Assess. 2006(130):1-145.
6. Jacobs I, Oram D, Fairbanks J, Turner J, Frost C, Grudzinskas JG. A risk of malignancy index incorporating CA 125, ultrasound and menopausal status for the accurate preoperative diagnosis of ovarian cancer. Br J Obstet Gynaecol. 1990;97(10):922-9.
7. Moore RG, McMeekin DS, Brown AK, DiSilvestro P, Miller MC, Allard WJ, et al. A novel multiple marker bioassay utilizing HE4 and CA125 for the prediction of ovarian cancer in patients with a pelvic mass. Gynecol Oncol. 2009;112(1):40-6.
8. Karlsen MA, Sandhu N, Høgdall C, Christensen IJ, Nedergaard L, Lundvall L, et al. Evaluation of HE4, CA125, risk of ovarian malignancy algorithm (ROMA) and risk of malignancy index (RMI) as diagnostic tools of epithelial ovarian cancer in patients with a pelvic mass. Gynecol Oncol. 2012;127(2):379-83.

9. Liest AL, Omran AS, Mikiver R, Rosenberg P, Uppugunduri S. RMI and ROMA are equally effective in discriminating between benign and malignant gynecological tumors: A prospective population-based study. Acta Obstet Gynecol Scand. 2019;98(1):24-33.

10. Van Gorp T, Cadron I, Despierre E, Daemen A, Leunen K, Amant F, et al. HE4 and CA125 as a diagnostic test in ovarian cancer: prospective validation of the Risk of Ovarian Malignancy Algorithm. Br J Cancer. 2011;104(5):863-70.

11. Lycke M, Kristjansdottir B, Sundfeldt K. A multicenter clinical trial validating the performance of HE4, CA125, risk of ovarian malignancy algorithm and risk of malignancy index. Gynecol Oncol. 2018;151(1):159-65.

12. Dayyani F, Uhlig S, Colson B, Simon K, Rolny V, Morgenstern D, et al. Diagnostic Performance of Risk of Ovarian Malignancy Algorithm Against CA125 and HE4 in Connection With Ovarian Cancer: A Meta-analysis. Int J Gynecol Cancer. 2016;26(9):1586-93.

13. Geng J, Fan H, Tang X, Zhai H, Zhang Z. Diversified pattern of the human colorectal cancer microbiome. Gut Pathog. 2013;5(1):2.

14. Schwabe RF, Jobin C. The microbiome and cancer. Nat Rev Cancer. 2013;13(11):800-12.

15. Bultman SJ. Emerging roles of the microbiome in cancer. Carcinogenesis. 2014;35(2):249-55.

16. Ahn J, Sinha R, Pei Z, Dominianni C, Wu J, Shi J, et al. Human gut microbiome and risk for colorectal cancer. J Nat Cancer Inst. 2013;105(24):1907-11.

17. Bhatt AP, Redinbo MR, Bultman SJ. The role of the microbiome in cancer development and therapy. CA Cancer J Cin. 2017;67(4):326-44.

18. Raza MH, Gul K, Arshad A, Riaz N, Waheed U, Rauf A, et al. Microbiota in cancer development and treatment. J Cancer Res Clin Oncol. 2019;145(1):49-63.

19. Kuehn MJ, Kesty NC. Bacterial outer membrane vesicles and the host-pathogen interaction. Genes Dev. 2005;19(22):2645-55.

20. Roier S, Zingl FG, Cakar F, Schild S. Bacterial outer membrane vesicle biogenesis: a new mechanism and its implications. Microb Cell. 2016;3(6):257-9.

21. Zhou B, Sun C, Huang J, Xia M, Guo E, Li N, et al. The biodiversity Composition of Microbiome in Ovarian Carcinoma Patients. Sci Rep. 2019;9(1):1691.

22. Rhee SJ, Kim H, Lee Y, Lee HJ, Park CHK, Yang J, et al. Comparison of serum microbiome composition in bipolar and major depressive disorders. J Psychiatr Res. 2020;123:31-8.

23. Kechin A, Boyarskikh U, Kel A, Filipenko M. cutPrimers: A New Tool for Accurate Cutting of Primers from Reads of Targeted Next Generation Sequencing. J Comput Biol. 2017;24(11):1138-43.

24. Bokulich NA, Subramanian S, Faith JJ, Gevers D, Gordon JI, Knight R, et al. Quality-filtering vastly improves diversity estimates from Illumina amplicon sequencing. Nat Methods. 2013;10(1):57-9.

25. Kwon S, Lee B, Yoon S. CASPER: context-aware scheme for paired-end reads from high-throughput amplicon sequencing. BMC Bioinformatics. 2014;15 Suppl 9(Suppl 9):S10.

26. Rognes T, Flouri T, Nichols B, Quince C, Mahé F. VSEARCH: a versatile open source tool for metagenomics. PeerJ. 2016;4:e2584.

27. Caporaso JG, Kuczynski J, Stombaugh J, Bittinger K, Bushman FD, Costello EK, et al. QIIME allows analysis of high-throughput community sequencing data. Nat Methods. 2010;7(5):335-6.

28. Pepper IL, Gerba CP, Gentry TJ. Environmental Microbiology, 3rd ed.; Academic press: San Diego, CA, USA, 2014.

29. Kinross JM, Darzi AW, Nicholson JK. Gut microbiome-host interactions in health and disease. Genome Med. 2011;3(3):14.

30. Clemente JC, Ursell LK, Parfrey LW, Knight R. The impact of the gut microbiota on human health: an integrative view. Cell. 2012;148(6):1258-70.

31. Walther-António MR, Chen J, Multinu F, Hokenstad A, Distad TJ, Cheek EH, et al. Potential contribution of the uterine microbiome in the development of endometrial cancer. Genome Med. 2016;8(1):122.

32. Peleg AY, Seifert H, Paterson DL. Acinetobacter baumannii: emergence of a successful pathogen. Clin Microbiol Rev. 2008;21(3):538-82.

33. Prabhash K, Medhekar A, Ghadyalpatil N, Noronha V, Biswas S, Kurkure P, et al. Blood stream infections in cancer patients: a single center experience of isolates and sensitivity pattern. Indian J Cancer. 2010;47(2):184-8.

34. Chiang MC, Kuo SC, Chen SJ, Yang SP, Lee YT, Chen TL, et al. Clinical characteristics and outcomes of bacteremia due to different genomic species of Acinetobacter baumannii complex in patients with solid tumors. Infection. 2012;40(1):19-26.

35. Takeuchi O, Akira S. Toll-like receptors; their physiological role and signal transduction system. Int Immunopharmacol. 2001;1(4):625-35.

36. Knapp S, Wieland CW, Florquin S, Pantophlet R, Dijkshoorn L, Tshimbalanga N, et al. Differential roles of CD14 and toll-like receptors 4 and 2 in murine Acinetobacter pneumonia. Am J Respir Crit Care Med. 2006;173(1):122-9.

37. Erridge C, Moncayo-Nieto OL, Morgan R, Young M, Poxton IR. Acinetobacter baumannii lipopolysaccharides are potent stimulators of human monocyte activation via Toll-like receptor 4 signalling. J Med Microbiol. 2007;56(Pt 2):165-71.

38. Kim CH, Jeong YJ, Lee J, Jeon SJ, Park SR, Kang MJ, et al. Essential role of toll-like receptor 4 in Acinetobacter baumannii-induced immune responses in immune cells. Microb Pathog. 2013;54:20-5.

39. Jun SH, Lee JH, Kim BR, Kim SI, Park TI, Lee JC, et al. Acinetobacter baumannii outer membrane vesicles elicit a potent innate immune response via membrane proteins. PloS One. 2013;8(8):e71751.

40. Nho JS, Jun SH, Oh MH, Park TI, Choi CW, Kim SI, et al. Acinetobacter nosocomialis secretes outer membrane vesicles that induce epithelial cell death and host inflammatory responses. Microb Pathog. 2015;81:39-45.

41. Zhou M, McFarland-Mancini MM, Funk HM, Husseinzadeh N, Mounajjed T, Drew AF. Toll-like receptor expression in normal ovary and ovarian tumors. Cancer Immunol Immunother. 2009;58(9):1375-85.

42. Kelly MG, Alvero AB, Chen R, Silasi DA, Abrahams VM, Chan S, et al. TLR-4 signaling promotes tumor growth and paclitaxel chemoresistance in ovarian cancer. Cancer Res. 2006;66(7):3859-68.

43. Sugiyama T, Okamoto A, Enomoto T, Hamano T, Aotani E, Terao Y, et al. Randomized Phase III Trial of Irinotecan Plus Cisplatin Compared With Paclitaxel Plus Carboplatin As First-Line Chemotherapy for Ovarian Clear Cell Carcinoma: JGOG3017/GCIG Trial. J Clin Oncol. 2016;34(24):2881-7.

44. Kim SI, Lim MC, Lim J, Won YJ, Seo SS, Kang S, et al. Incidence of epithelial ovarian cancer according to histologic subtypes in Korea, 1999 to 2012. J Gynecol Oncol. 2016;27(1):e5.

45. Smith LH, Morris CR, Yasmeen S, Parikh-Patel A, Cress RD, Romano PS. Ovarian cancer: can we make the clinical diagnosis earlier? Cancer. 2005;104(7):1398-407.

46. Cho KR, Shih Ie M. Ovarian cancer. Annu Rev Pathol. 2009;4:287-313.

47. Bristow RE, Tomacruz RS, Armstrong DK, Trimble EL, Montz FJ. Survival effect of maximal cytoreductive surgery for advanced ovarian carcinoma during the platinum era: a meta-analysis. J Clin Oncol. 2002;20(5):1248-59.

48. Chi DS, Franklin CC, Levine DA, Akselrod F, Sabbatini P, Jarnagin WR, et al. Improved optimal cytoreduction rates for stages IIIC and IV epithelial ovarian, fallopian tube, and primary peritoneal cancer: a change in surgical approach. Gynecol Oncol. 2004;94(3):650-4.

49. Wimberger P, Wehling M, Lehmann N, Kimmig R, Schmalfeldt B, Burges A, et al. Influence of residual tumor on outcome in ovarian cancer patients with FIGO stage IV disease: an exploratory analysis of the AGO-OVAR (Arbeitsgemeinschaft Gynaekologische Onkologie Ovarian Cancer Study Group). Ann Surg Oncol. 2010;17(6):1642-8.

50. Cannistra SA. Cancer of the ovary. N Engl J Med. 2004;351(24):2519-29.

51. Teramukai S, Ochiai K, Tada H, Fukushima M. PIEPOC: a new prognostic index for advanced epithelial ovarian cancer--Japan Multinational Trial Organization OC01-01. J Clin Oncol. 2007;25(22):3302-6.

52. Chi DS, Palayekar MJ, Sonoda Y, Abu-Rustum NR, Awtrey CS, Huh J, et al. Nomogram for survival after primary surgery for bulky stage IIIC ovarian carcinoma. Gynecol Oncol. 2008;108(1):191-4.

53. Gerestein CG, Eijkemans MJ, de Jong D, van der Burg ME, Dykgraaf RH, Kooi GS, et al. The prediction of progression-free and overall survival in women with an advanced stage of epithelial ovarian carcinoma. BJOG. 2009;116(3):372-80.

54. Barlin JN, Yu C, Hill EK, Zivanovic O, Kolev V, Levine DA, et al. Nomogram for predicting 5-year disease-specific mortality after primary surgery for epithelial ovarian cancer. Gynecol Oncol. 2012;125(1):25-30.

55. Lee CK, Simes RJ, Brown C, Lord S, Wagner U, Plante M, et al. Prognostic nomogram to predict progression-free survival in patients with platinum-sensitive recurrent ovarian cancer. Br J Cancer. 2011;105(8):1144-50.

56. Lee CK, Simes RJ, Brown C, Gebski V, Pfisterer J, Swart AM, et al. A prognostic nomogram to predict overall survival in patients with platinum-sensitive recurrent ovarian cancer. Ann Oncol. 2013;24(4):937-43.

57. Previs RA, Bevis KS, Huh W, Tillmanns T, Perry L, Moore K, et al. A prognostic nomogram to predict overall survival in women with recurrent ovarian cancer treated with bevacizumab and chemotherapy. Gynecol Oncol. 2014;132(3):531-6.

58. Paik ES, Sohn I, Baek SY, Shim M, Choi HJ, Kim TJ, et al. Nomograms Predicting Platinum Sensitivity, Progression-Free Survival, and Overall Survival Using Pretreatment Complete Blood Cell Counts in Epithelial Ovarian Cancer. Cancer Res Treat. 2017;49(3):635-42.

59. Foote J, Lopez-Acevedo M, Samsa G, Lee PS, Kamal AH, Alvarez Secord A, et al. Predicting 6- and 12-Month Risk of Mortality in Patients With

Platinum-Resistant Advanced-Stage Ovarian Cancer: Prognostic Model to Guide Palliative Care Referrals. Int J Gynecol Cancer. 2018;28(2):302-7.

60. Eisenhauer EA, Therasse P, Bogaerts J, Schwartz LH, Sargent D, Ford R, et al. New response evaluation criteria in solid tumours: revised RECIST guideline (version 1.1). Eur J Cancer. 2009;45(2):228-47.

61. Rustin GJ, Vergote I, Eisenhauer E, Pujade-Lauraine E, Quinn M, Thigpen T, et al. Definitions for response and progression in ovarian cancer clinical trials incorporating RECIST 1.1 and CA 125 agreed by the Gynecological Cancer Intergroup (GCIG). Int J Gynecol Cancer. 2011;21(2):419-23.

62. Heagerty PJ, Zheng Y. Survival model predictive accuracy and ROC curves. Biometrics. 2005;61(1):92-105.

63. Mantovani A, Allavena P, Sica A, Balkwill F. Cancer-related inflammation. Nature. 2008;454(7203):436-44.

64. Pujade-Lauraine E, Hilpert F, Weber B, Reuss A, Poveda A, Kristensen G, et al. Bevacizumab combined with chemotherapy for platinum-resistant recurrent ovarian cancer: The AURELIA open-label randomized phase III trial. J Clin Oncol. 2014;32(13):1302-8.

65. Aghajanian C, Blank SV, Goff BA, Judson PL, Teneriello MG, Husain A, et al. OCEANS: a randomized, double-blind, placebo-controlled phase III trial of chemotherapy with or without bevacizumab in patients with platinum-sensitive recurrent epithelial ovarian, primary peritoneal, or fallopian tube cancer. J Clin Oncol. 2012;30(17):2039-45.

66. Coleman RL, Brady MF, Herzog TJ, Sabbatini P, Armstrong DK, Walker JL, et al. Bevacizumab and paclitaxel-carboplatin chemotherapy and secondary cytoreduction in recurrent, platinum-sensitive ovarian cancer (NRG Oncology/Gynecologic Oncology Group study GOG-0213): a multicentre, open-label, randomised, phase 3 trial. Lancet Oncol. 2017;18(6):779-91.

67. Pujade-Lauraine E, Ledermann JA, Selle F, Gebski V, Penson RT, Oza AM, et al. Olaparib tablets as maintenance therapy in patients with platinum-sensitive, relapsed ovarian cancer and a BRCA1/2 mutation

(SOLO2/ENGOT-Ov21): a double-blind, randomised, placebo-controlled, phase 3 trial. Lancet Oncol. 2017;18(9):1274-84.

68. Cruz-Jentoft AJ, Bahat G, Bauer J, Boirie Y, Bruyère O, Cederholm T, et al. Sarcopenia: revised European consensus on definition and diagnosis. Age Ageing. 2019;48(1):16-31.

69. Caan BJ, Cespedes Feliciano EM, Prado CM, Alexeeff S, Kroenke CH, Bradshaw P, et al. Association of Muscle and Adiposity Measured by Computed Tomography With Survival in Patients With Nonmetastatic Breast Cancer. JAMA Oncol. 2018;4(6):798-804.

70. Kim EY, Kim YS, Park I, Ahn HK, Cho EK, Jeong YM. Prognostic Significance of CT-Determined Sarcopenia in Patients with Small-Cell Lung Cancer. J Thorac Oncol. 2015;10(12):1795-9.

71. Fukushima H, Yokoyama M, Nakanishi Y, Tobisu K, Koga F. Sarcopenia as a prognostic biomarker of advanced urothelial carcinoma. PloS One. 2015;10(1):e0115895.

72. Lee JS, Kim YS, Kim EY, Jin W. Prognostic significance of CT-determined sarcopenia in patients with advanced gastric cancer. PloS One. 2018;13(8):e0202700.

73. Kumar A, Moynagh MR, Multinu F, Cliby WA, McGree ME, Weaver AL, et al. Muscle composition measured by CT scan is a measurable predictor of overall survival in advanced ovarian cancer. Gynecol Oncol. 2016;142(2):311-6.

74. Bronger H, Hederich P, Hapfelmeier A, Metz S, Noël PB, Kiechle M, et al. Sarcopenia in Advanced Serous Ovarian Cancer. Int J Gynecol Cancer. 2017;27(2):223-32.

75. Rutten IJ, Ubachs J, Kruitwagen RF, van Dijk DP, Beets-Tan RG, Massuger LF, et al. The influence of sarcopenia on survival and surgical complications in ovarian cancer patients undergoing primary debulking surgery. Eur J Surg Oncol. 2017;43(4):717-24.

76. Staley SA, Tucker K, Newton M, Ertel M, Oldan J, Doherty I, et al. Sarcopenia as a predictor of survival and chemotoxicity in patients with

epithelial ovarian cancer receiving platinum and taxane-based chemotherapy. Gynecol Oncol. 2020;156(3):695-700.

77. OECD Health Statistic. 2019. Available online: http://www.oecd.org/els/health-systems/health-data.htm (accessed on 22 February 2020).

78. Mourtzakis M, Prado CM, Lieffers JR, Reiman T, McCargar LJ, Baracos VE. A practical and precise approach to quantification of body composition in cancer patients using computed tomography images acquired during routine care. Appl Physiol Nutr Metab. 2008;33(5):997-1006.

79. Shen W, Punyanitya M, Wang Z, Gallagher D, St-Onge MP, Albu J, et al. Total body skeletal muscle and adipose tissue volumes: estimation from a single abdominal cross-sectional image. J Appl Physiol (1985). 2004;97(6):2333-8.

80. WHO Expert Consultation. Appropriate body-mass index for Asian populations and its implications for policy and intervention strategies. Lancet. 2004;363(9403):157-63.

81. Aubrey J, Esfandiari N, Baracos VE, Buteau FA, Frenette J, Putman CT, et al. Measurement of skeletal muscle radiation attenuation and basis of its biological variation. Acta Physiol (Oxf). 2014;210(3):489-97.

82. Nishikawa H, Shiraki M, Hiramatsu A, Moriya K, Hino K, Nishiguchi S. Japan Society of Hepatology guidelines for sarcopenia in liver disease (1st edition): Recommendation from the working group for creation of sarcopenia assessment criteria. Hepatol Res. 2016;46(10):951-63.

83. Hamaguchi Y, Kaido T, Okumura S, Kobayashi A, Shirai H, Yao S, et al. Proposal for new selection criteria considering pre-transplant muscularity and visceral adiposity in living donor liver transplantation. J Cachexia Sarcopenia Muscle. 2018;9(2):246-54.

84. Fearon K, Strasser F, Anker SD, Bosaeus I, Bruera E, Fainsinger RL, et al. Definition and classification of cancer cachexia: an international consensus. Lancet Oncol. 2011;12(5):489-95.

85. Feng Z, Wen H, Ju X, Bi R, Chen X, Yang W, et al. The preoperative prognostic nutritional index is a predictive and prognostic factor of high-grade serous ovarian cancer. BMC Cancer. 2018;18(1):883.

86. Levolger S, van Vugt JL, de Bruin RW, JN IJ. Systematic review of sarcopenia in patients operated on for gastrointestinal and hepatopancreatobiliary malignancies. Br J Surg. 2015;102(12):1448-58.

87. Shachar SS, Williams GR, Muss HB, Nishijima TF. Prognostic value of sarcopenia in adults with solid tumours: A meta-analysis and systematic review. Eur J Cancer. 2016;57:58-67.

88. Nakayama N, Nakayama K, Nakamura K, Razia S, Kyo S. Sarcopenic Factors May Have No Impact on Outcomes in Ovarian Cancer Patients. Diagnostics (Basel). 2019;9(4):206.

89. Gadducci A, Cosio S, Fanucchi A, Genazzani AR. Malnutrition and cachexia in ovarian cancer patients: pathophysiology and management. Anticancer Res. 2001;21(4B):2941-7.

90. Kim SI, Kim HS, Kim TH, Suh DH, Kim K, No JH, et al. Impact of underweight after treatment on prognosis of advanced-stage ovarian cancer. J Immunol Res. 2014;2014:349546.

91. Lee K, Shin Y, Huh J, Sung YS, Lee IS, Yoon KH, et al. Recent Issues on Body Composition Imaging for Sarcopenia Evaluation. Korean J Radiol. 2019;20(2):205-17.

92. Antoun S, Lanoy E, Iacovelli R, Albiges-Sauvin L, Loriot Y, Merad-Taoufik M, et al. Skeletal muscle density predicts prognosis in patients with metastatic renal cell carcinoma treated with targeted therapies. Cancer. 2013;119(18):3377-84.

93. Martin L, Birdsell L, Macdonald N, Reiman T, Clandinin MT, McCargar LJ, et al. Cancer cachexia in the age of obesity: skeletal muscle depletion is a powerful prognostic factor, independent of body mass index. J Clin Oncol. 2013;31(12):1539-47.

94. Baracos VE, Arribas L. Sarcopenic obesity: hidden muscle wasting and its impact for survival and complications of cancer therapy. Ann Oncol. 2018;29(suppl_2):ii1-9.

95. Malietzis G, Currie AC, Athanasiou T, Johns N, Anyamene N, Glynne-Jones R, et al. Influence of body composition profile on outcomes following colorectal cancer surgery. Br J Surg. 2016;103(5):572-80.

96. Kim B, Kim HS, Kim S, Haegeman G, Tsang BK, Dhanasekaran DN, et al. Adipose Stromal Cells from Visceral and Subcutaneous Fat Facilitate Migration of Ovarian Cancer Cells via IL-6/JAK2/STAT3 Pathway. Cancer Res Treat. 2017;49(2):338-49.

97. Wisse BE. The inflammatory syndrome: the role of adipose tissue cytokines in metabolic disorders linked to obesity. J Am Soc Nephrol. 2004;15(11):2792-800.

98. Dalle S, Rossmeislova L, Koppo K. The Role of Inflammation in Age-Related Sarcopenia. Front Physiol. 2017;8:1045.

99. Dent E, Morley JE, Cruz-Jentoft AJ, Arai H, Kritchevsky SB, Guralnik J, et al. International Clinical Practice Guidelines for Sarcopenia (ICFSR): Screening, Diagnosis and Management. J Nutr Health Aging. 2018;22(10):1148-61.

100. Burton LA, Sumukadas D. Optimal management of sarcopenia. Clin Interv Aging. 2010;5:217-28.

101. Rolland Y, Czerwinski S, Abellan Van Kan G, Morley JE, Cesari M, Onder G, et al. Sarcopenia: its assessment, etiology, pathogenesis, consequences and future perspectives. J Nutr Health Aging. 2008;12(7):433-50.

102. Dalakas MC. Inflammatory muscle diseases. N Engl J Med. 2015;372(18):1734-47.

103. Seabolt LA, Welch EB, Silver HJ. Imaging methods for analyzing body composition in human obesity and cardiometabolic disease. Ann N Y Acad Sci. 2015;1353:41-59.

104. Erlandson MC, Lorbergs AL, Mathur S, Cheung AM. Muscle analysis using pQCT, DXA and MRI. Eur J Radiol. 2016;85(8):1505-11.

국문 초록

상피성 난소암의 진단 및 예후 예측을 위한 다차원 모델 개발 연구

김 세 익

서울대학교 대학원

의학과 산부인과학 전공

난소암은 여성에서 발생하는 암종 중 사망률이 높은 치명적인 암종으로, 부인암 중 가장 낮은 5년 생존률을 보인다. 암 특이적인 증상과 효과적인 스크리닝 도구가 없는 까닭에 난소암은 진행성 병기에 진단되는 경향이 있고, 이로 인해 치료에도 불구 높은 재발률과 사망률을 보인다. 현재, 진행성 병기의 상피성 난소암의 1차 치료는 종양감축수술과 백금 기반 항암화학요법으로 정립되어 있다. 그럼에도 불구하고, 80%의 환자는 결국 난소암의 재발을 겪게 된다.

정밀의학 시대에 발맞춰 난소암에 대한 정확한 진단 모델과 예후 예측 모델의 발굴이 난소암 환자에 있어 맞춤 치료 구현의 첫 걸음이라 할 수 있겠다. 따라서 상피성 난소암에 대한 다양한 모델을 개발하는 일련의 연구들을 수행하였다.

먼저, 챕터 1 에서는 혈액 내 마이크로비옴 유래 세포밖 소포체의 메타지놈 데이터를 이용하는 난소암과 양성난소종양 감별 진단 모델을 개발하였다.

자궁 부속기 종괴가 발견된 여성에서 난소암과 양성난소종양을 구분하는 것은, 수술의 방법 등 치료 계획을 결정하는데 있어 매우 중요한 문제다. 현재 난소암 진단을 위한 도구로는 혈액 종양표지자인 CA-125와 초음파, 컴퓨터단층촬영(CT) 스캔, 자기공명영상(MRI)

등의 영상 검사가 있다. 하지만, 정확도 측면에서 보다 높은 정확도의 난소암 진단 도구 개발이 절실한 실정이다.

본 연구에서는 병리학적으로 확인된 난소암 환자 166명과 양성난소종양 환자 76명의 혈액 샘플을 이용하였다. 모델 개발 단계와 검증 단계로 표본들을 2:1 무작위 배정하였다. 환자의 혈청으로부터 마이크로비옴 유래 세포밖 소포체를 분리하고 16S rDNA amplicon sequencing을 수행하였다. 메타지놈 분석 결과, 난소암 환자 그룹과 양성난소종양 환자 그룹은 유의하게 다른 조성을 보였다. 양성난소종양 환자 그룹 대비 난소암 환자 그룹에서 아시네토박터 속(genus) 균이 더 풍부하게 확인되었다. 메타지놈과 임상병리학적 변수들을 조합하여 만든 여러 난소암 진단 모델 중 나이와 혈액 종양표지자인 CA-125, 그리고 아시네토박터의 상대존재비로 구성된 모델이 가장 높은 진단 성능을 보였다. 해당 모델의 수신기 작동 특성 곡선 아래 영역 (AUC) 값은 모델 개발 단계와 검증 단계에서 각각 0.898 과 0.846으로 확인되었다. 따라서, 본 연구 결과는 난소암 진단을 위한 잠재적인 도구로서 혈청 마이크로비옴 유래 세포밖 소포체의 메타지놈 분석의 가능성을 확인하였다.

챕터 2 에서는 상피성 난소암 환자의 치료반응과 예후를 예측하는 노모그램들을 개발하였다.

현재까지 CT 스캔, 혈액 종양표지자, 수술소견, 병리학적 검사결과 등을 기반으로 상피성 난소암의 생존을 예측하는 여러 모델들이 개발된 바 있다. 하지만, 선행 모델들은 각기 다른 연구 대상 집단에서 개발되었으며, 여러 임상병리학적 요인 중 단편만을 분석하였으며, 예측 능력이 낮거나 제한적이어서 임상의사가 실제 진료 현장에서 활용하기 어려웠다. 따라서, 본 연구는 국내 두 3차 의료기관으로부터 다량의 임상병리학적 데이터를 획득하고 통합적인 통계분석을 통해 보다 정밀한 치료반응 및 생존 예후를 예측하는 노모

그램을 개발하는 것을 목적으로 하였다. 이전에 발표된 바 있는, 그리고 잠재적 가능성이 있는 모든 예후 요인들을 포함하여 분석하였다.

백금 민감성, 3년 무진행생존률 및 5년 전체생존률을 예측하는 새로 개발된 노모그램의 AUC 값은 각각 0.758, 0.841, 0.805 이었다. 난소암 치료 시 선행항암화학요법을 시행한 환자들을 제외하고 1차 종양감축수술을 받은 환자들에게만 국한된 예측 노모그램도 개발하였다. 이 경우 백금 민감성, 3년 무진행생존률 및 5년 전체생존률을 예측하는 새로 개발된 노모그램의 AUC 값은 각각 0.713, 0.839, 0.803 이었다. 결론적으로 상피 난소암 환자의 치료 반응과 생존 예후를 예측하는 노모그램 개발에 성공하였다. 각각의 노모그램들은 실제 진료 현장과 임상시험 설계 등에서 유용하게 활용될 것으로 예상된다.

챕터 3 에서는 진행성 병기의 고등급 장액성 난소암 환자를 대상으로 근감소증과 신체 구성이 생존 예후에 미치는 영향을 탐색하였다.

골격근의 질량과 기능의 상실로 정의되는 근감소증이 암질환의 예후에 미치는 영향은 지역과 인종에 따라 다를 수 있다. 최근에는 라디오믹스로 불리는 영상 검사를 이용한 정량적 분석 방법이 임상 결정 및 환자 층화에 있어 유용한 접근법으로 떠오르고 있다. 세 번째 요추(L3) 레벨의 CT 스캔 단면 영상은 골격근육과 지방조직, 지방분포 등 개인의 신체 구성을 잘 반영하여 나타내는 것으로 알려져 있다.

본 연구에서는 한국인 FIGO 병기 III-IV 기의 고등급 장액성 난소암 환자의 진단 당시 촬영한 CT 스캔으로 붙어 L3 레벨의 골격근 지수 (skeletal muscle index, SMI)를 측정하였다. 근감소증은 SMI 값이 39.0 cm^2/m^2 미만 일 때로 정의하였을 때 76명은 근감소

증 그룹, 103명은 대조군으로 확인되었다. 근감소증 존재 유무에 따라 두 군 간 환자의 임상병리학적 특성과 생존 결과를 비교하였다. 두 군 간 동반질환, 병기, CA-125, 수술 후 잔존종양의 크기는 차이가 없었다. 두 군은 또한 유사한 무진행생존기간과 전체생존기간을 보였다. 근감소증 그룹 내에서 같은 단면영상에서 측정한 지방 대 근육 비 (fat-to-muscle ratio, FMR) 에 따라 FMR 이 높은 (2.1 이상, 38명) 과 낮은 (2.1 미만, 38명) 두 그룹으로 세분화 하여 분석을 하였다. 그 결과, 높은 FMR 그룹이 낮은 FMR 그룹 대비 통계적으로 유의하게 불량한 5년 전체생존률을 보였다 (44.7% vs. 80.0%; P=0.046). 하지만 무진행생존기간은 차이가 없었다 (P=0.365). 다변량분석 결과 높은 FMR 값이 전체생존기간에 대한 통계적으로 유의하게 불량한 예후 인자임을 확인하였다 (보정 위험비, 3.377; 95% 신뢰구간, 1.170–9.752; P=0.024). 결론적으로, 한국인 진행성 병기의 고등급 장액성 난소암 환자에서 근감소증 자체는 재발률이나 생존률에 영향을 주지 않았으나, 높은 지방 대 근육 비가 불량한 생존률과 연관이 있음을 확인할 수 있었다.

상기 기술한 바와 같이, 상피성 난소암에서 각 개인의 임상병리학적, 메타지노믹스, 그리고 라디오믹스 데이터를 통합 분석함으로써 다양한 진단 및 예측 모델을 성공적으로 개발하였다. 다차원적 분석 방법으로 상피성 난소암에서의 각 모델의 예측 능력을 향상시킴으로써 암 정밀의학 분야에 있어 중요한 접근 방법임을 확인할 수 있었다. 이러한 접근방식을 통해 난소암 환자에게 개별화된 맞춤 치료를 구현할 수 있을 것으로 기대된다.

주요어: 난소암, 진단, 예후, 치료 반응, 생존, 세포밖 소포체, 마이크로비옴, 메타지놈 분석, 근감소증, 신체 구성

학 번 : 2014-30620